To the Graduate Council:

I am submitting herewith a thesis written by Thomas Wesley Kerlin III entitled "Explicit Calibration of an Electro-Optical Aerosol Monitor." I recommend that it be accepted in partial fulfillment of the requirements for the degree of Master of Science, with a major in Electrical Engineering.

Frederick Shofner, Major Professor

We have read this thesis
and recommend its acceptance:

Accepted for the Council:

Vice Chancellor
Graduate Studies and Research

Thesis
80
.K474
cop. 2

EXPLICIT CALIBRATION OF AN ELECTRO-OPTICAL AEROSOL MONITOR

A Thesis

Presented for the

Master of Science

Degree

The University of Tennessee, Knoxville

Thomas Wesley Kerlin III

March 1980

111824

ACKNOWLEDGMENTS

The author is indebted to Dr. Gerhard Kreikebaum and Arthur C. Miller, Jr., of PPM, Inc., for their technical guidance and helpful suggestions.

The author would like to express appreciation to Dr. Frederick M. Shofner for support and encouragement through the course of this research.

Dr. Kermit E. Duckett is acknowledged for his constructive contributions and the use of laboratory facilities.

Gratitude is expressed to Dr. J. M. Googe for providing the author with a teaching assistantship and PPM, Inc., for financial support.

Judy Armstrong is thanked for her time and skill in typing drafts of this thesis.

Finally, the author expresses gratitude to his wife, Candice, for continued support, encouragement, and understanding and for preparation of the figures contained in this manuscript, and to his parents for their positive influences.

ABSTRACT

An electro-optical method of measuring particulate mass concentration and approximate size distribution is described with emphasis on calibration procedures. The Continuous Aerosol Monitor (CAM), a microprocessor-based, forward-scattering electro-optical instrument, is characterized for cotton dust particles in textile mills. Optical microscopy is utilized in determining the cotton dust characteristics to provide insight into and calibration for a unique compensation technique implemented in the CAM microprocessor to compute large particle mass. Geometrical properties of cotton fibers verify the experimentally determined form of the large particle compensation algorithm. Pulse height analyzer calibration is established on both a number and mass basis. The resulting calibration curve slopes are in agreement with theoretical system response. Also, vertical elutriator penetration efficiency is determined.

TABLE OF CONTENTS

CHAPTER		PAGE
I.	INTRODUCTION	1
II.	SYSTEM DESCRIPTION AND THEORY OF OPERATION	6
III.	EXPERIMENTAL METHODS	13
	Microscopic Analysis	13
	Equal Area Sampling	16
	Data Interpretation	19
	Fiber Orientation	25
	Relationship between Stokes Diameter and Projected Diameter	28
IV.	EXPERIMENTAL RESULTS	33
	Overview	33
	Penetration Efficiency Calibration	34
	CAM Mass Calibration	46
	CAM Counting Efficiency	57
	Volume to Area Ratio	60
V.	SUMMARY AND CONCLUSIONS	63
LIST OF REFERENCES		67
APPENDIX		70
VITA		72

LIST OF FIGURES

FIGURE		PAGE
2-1.	CAM System Block Diagram.	7
2-2.	Forward Scattered Power vs. α	9
2-3.	Response per Unit Mass vs. $\bar{d}_m$ Mass Mean Diameter for CAM with Large Particle Compensation.	10
3-1.	Filter Sections for Equal Area Sampling	20
3-2.	Fiber Orientation Geometry.	27
3-3.	Ratio of Stokes Diameter to Projected Diameter vs. Aspect Ratio, β	31
4-1.	Typical p(d), p'(d), and F(d) Curves.	36
4-2.	Penetration Efficiency Functions by Optical Microscopy. .	38
4-3.	Penetration Efficiency Functions by CAM Output Data . . .	39
4-4.	System Calibration by Penetration Efficiency Method . . .	41
4-5.	Vertical Elutriator Penetration Efficiency Function by CAM Output Data.	42
4-6.	Vertical Elutriator Penetration Efficiency Function by Optical Microscopy	44
4-7.	Vertical Elutriator Penetration Efficiency for Maximum and Minimum Particle Dimensions	45
4-8.	Mass Histograms from CAM PHA Data	50
4-9.	Mass Histograms from Optical Microscopy	51
4-10.	Cumulative Mass Distributions by Optical Microscopy . . .	52
4-11.	Cumulative CAM PHA Distribution	54
4-12.	CAM PHA Channel Calibration on a Mass Basis	56
4-13.	CAM Counting Efficiency vs. PHA Channel	58
4-14.	CAM Counting Efficiency vs. Particle Count Rate	59
4-15.	Average Volume to Area Ratio for Cotton Dust.	61
A-1.	CAM Sensor and Control/Readout Unit	71

CHAPTER I

INTRODUCTION

The quantitative measurement of industrial emissions is rapidly becoming a unique engineering field in itself, encompassing a wide spectrum of applications. With new EPA and OSHA standards, it is important that cost-effective methods of monitoring industrial environments be developed.

It is known that a wide variety of airborne particulates are responsible for disease and even death in employees with prolonged exposure. Since emissions cannot generally be totally eliminated from the workplace, OSHA has determined maximum permissible exposure limits (PELs) for various aerosols. Periodic surveys are performed to insure that the OSHA standards are met. If violations are detected, the company is required by law to install or modify existing air purification equipment so that the condition is improved.

In the textile industry, prolonged exposure to cotton dust has been positively correlated with incidence of byssinosis, a disabling disease of the respiratory system (1). This disease is commonly referred to as "brown lung" in the cotton industry. Presently, OSHA has set the maximum allowable exposure to "lint-free" cotton dust at 200 $\mu g/m^3$, averaged over an 8-hour shift (2). The term "lint-free" is a subject of controversy among cotton dust researchers in that all conventional measurement schemes cannot totally exclude large fibrous material from the dust sample. By definition, respirable dust is composed of particles with equivalent Stokes diameters less than 15 μm. Physiological research

has shown that particles larger than this size are filtered out in the tracheal system and do not reach the lungs. Therfore, any mass associated with these large particles should theoretically be subtracted from the total mass, giving the "lint-free" respirable portion of the dust sample.

The accepted primary method of measuring cotton dust mass concentrations involves a gravimetric technique using the vertical elutriator (VE) (3). An aerodynamic preseparator, the vertical elutriator is designed to eliminate particles with Stokes diameters greater than 15 μm so that a "lint-free" sample of the ambient air is obtained at the outlet. This sample air is passed through a porous filter material at the top of the elutriator where the particles are deposited. The net increase in filter weight due to deposition of dust particles divided by the total volume of sampled air gives the average mass concentration $\bar{\chi}$ in $\mu g/m^3$.

Simple and reliable, the vertical elutriator is an obvious choice in primary methods. However, there are drawbacks to this method that motivate research into alternative techniques. First, it is known that the vertical elutriator does not perfectly exclude nonrespirable particles. These large particulates can have a significant effect upon the measured value of χ. Second, the VE is a labor intensive method requiring a large number of manhours for performing a plant-wide survey of dust concentrations. Third, results are susceptible to operator errors, as the filters must typically be weighed to within 10 μg on sensitive "micro-balance" scales.

Clearly, a semiautomatic instrument that could accurately determine mass concentration continuously and cost effectively would be beneficial

to the textile industry as well as others utilizing similar measurement techniques.

As an equivalent method of measuring aerosol mass concentrations, several different approaches have been attempted. One method utilizes the properties of piezoelectric crystals to determine the mass concentration. The change in resonant frequency due to deposition of particles on the surface of an oscillating piezoelectric crystal has been shown to be proportional to the mass concentration. Thermo-Systems, Incorporated (TSI), St. Paul, Minnesota, has developed a mass concentration monitor with a reported concentration range of 1-200,000 $\mu g/m^3$ (4). However, no size information is available from this method so that in effect the preseparator, typically an impaction device such as a cyclone determines the accuracy of "lint-free" respirable dust concentrations.

Another method, similar to turbidimetric techniques, is β-attenuation. The attenuation of a beam of β-radiation passing through a sample of deposited particles is shown to be related to the mass concentration (5). GCA of Bedford, Massachusetts, manufactures a portable unit with a measurement range of 1-50,000 $\mu g/m^3$. Again, no size information is implied from this method.

In order to obtain size characteristics, the particles must be weighed individually instead of collectively. To this effect, ppm, Inc., Knoxville, Tennessee, has developed a continuous *in situ* electro-optical sensor which measures mass concentration and is capable of distinguishing individual large particles. Utilizing forward scattering of infrared radiation, the Continuous Aerosol Monitor (CAM) is basically a transducer that produces an output voltage proportional to

the size of the scattering particle (6). Thus, for an ensemble of various size particles, the CAM analog output can be related to the instantaneous mass concentration of the sample. In addition, the distribution of output voltage is found to approximate the distribution of particle size so that a qualitative as well as quantitative measure of mass concentration is determined. The CAM optical sensor and control/readout unit are shown in the Appendix.

Prior work at ppm established methods of compensation for inherent underweighing of large particles by light-scattering means. These methods were applied to cotton dust implicitly; that is, the coefficients in the microprocessor algorithm were adjusted such that the readings of the CAM sensor best agreed with the reference gravimetric method.

It was recognized that the compensation scheme depended on the ability of the equipment to separate small and large particles so that the inherent underweighing of large particles could be compensated. It was also recognized that the average sensor response would be proportional to average particle projected area.

In this approach, the particle size calibration of the CAM was determined utilizing microscopic analysis, and the CAM response in pulse height analyzed form was correlated directly to the microscopically determined size distribution. The CAM mass response was also determined for respirable dust calculations. Other factors, such as sampling efficiency and sources of error, are examined. As a sidelight, the vertical elutriator is characterized and compared to the idealized model.

In Chapter II, the basic theory of operation of the CAM system is described. The major results of Mie scattering theory are given

without lengthy theoretical digression, as they are well documented elsewhere (7,8). System architecture is briefly outlined with a description of large particle compensation implemented in the microprocessor unit.

Chapter III deals with methods utilized in determining particle distributions. Microscopic analysis techniques are discussed and typical procedures are suggested. Approximations based on simple theories are explained with experimental justification.

The results of system calibration are given in Chapter IV. Two separate determinations were performed using different parameters as a basis of calibration. CAM sampling efficiency is computed, and overall instrument performance is discussed. Other interesting findings are briefly examined, and salient conclusions are summarized.

CHAPTER II

SYSTEM DESCRIPTION AND THEORY OF OPERATION

The basic components of the CAM system are shown schematically in Figure 2-1. A collimated beam of infrared radiation (λ = .904 μm) is produced by the light-emitting diode and beam-forming optics and is directed through the vertical elutriator effluent. An off-axis detector and collection optics determine the optically defined sampling volume. The detector output voltage is amplified and conditioned into a form compatible with the microprocessor input port. The microprocessor is programmed to store the particle data and perform mass concentration computations. An analog output signal representing the instantaneous mass concentration is obtained using a D/A converter. When a particle is present in the sampling volume, a voltage pulse is produced that is related to the physical characteristics of the particle. When a large number of particles are present in the sampling volume, a superposition of all the individual responses is indicated.

It is intuitive that the output voltage response is an increasing function of particle size. The exact relationship between scattering intensity and particle size is found in the theory of Mie (9,10). Basically, the scattering intensity function of a sphere in the path of a plane electro-magnetic wave is determined by applying Maxwell's equations with the appropriate boundary conditions. It is found that the solution to this problem is a complex function of particle diameter, refractive index, wavelength of illuminating radiation, and scattering angle. However, for a given optical configuration and particle material,

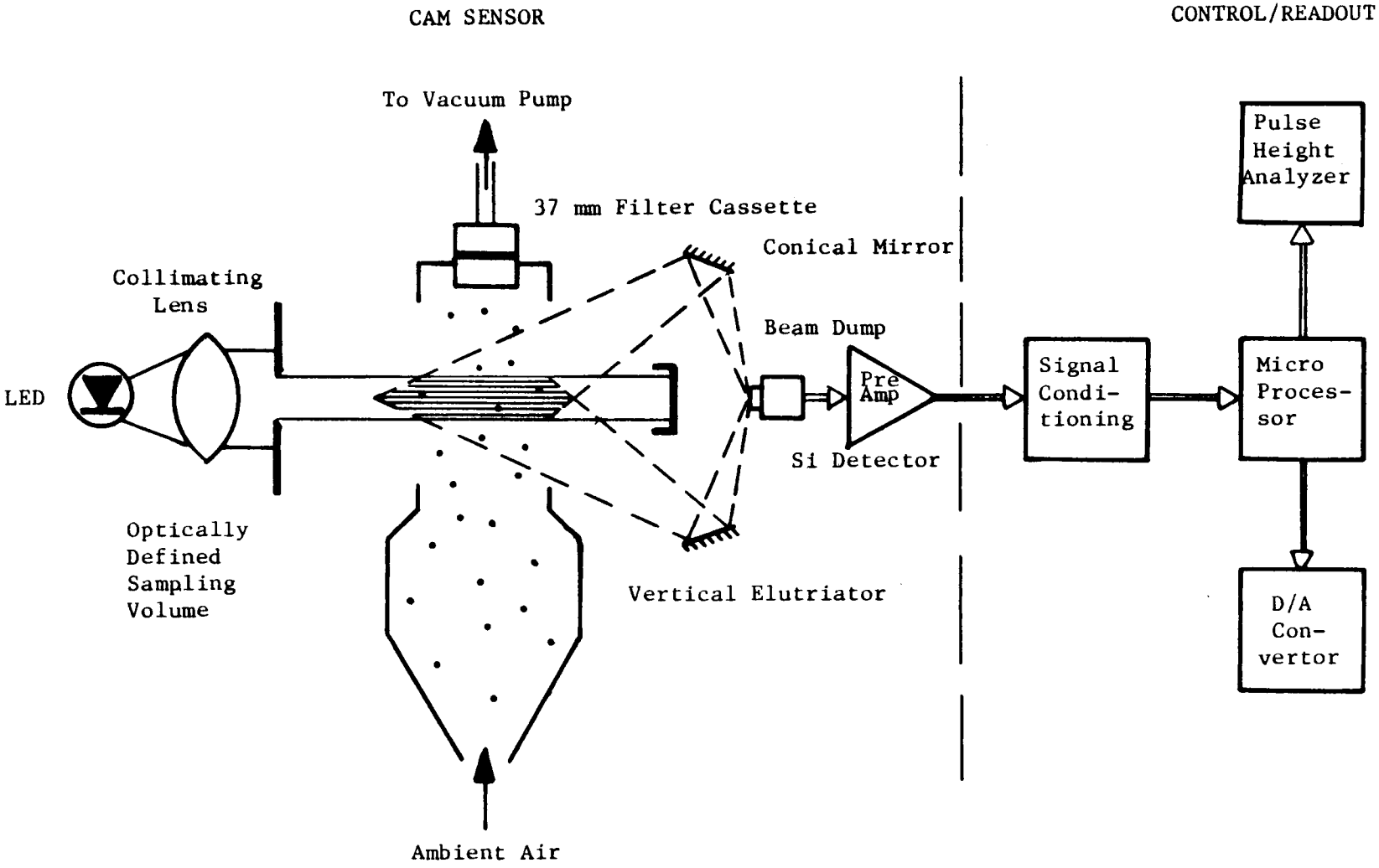


Figure 2-1. CAM system block diagram.

the particle diameter alone determines the response. Using typical values, computer simulations yield scattering curves, such as Figure 2-2 (7). The abscissa is proportional to particle diameter, and the ordinate is representative of scattered power. The dimensionless parameter α is given by:

$$\alpha = \frac{\pi d}{\lambda}. \tag{2-1}$$

It is apparent that three different response regions exist. For very large diameters, the scattered response goes as d^2 or area. For intermediate sizes ($5 < \alpha < 50$), the response is approximately proportional to d^3 or volume. A d^6 dependence is observed for very small diameters.

For a multiplicity of particles, the distribution is weighted by the individual scattering response and integrated over all diameters. The result is proportional to the total scattered power. The response per unit volume is found by dividing the total scattered power by the third moment (or volume) of the distribution. For log-normal distributions with a given geometric standard deviation σ_g and variable mean diameters $\overline{d}_m$, curves, such as shown in Figure 2-3, are generated (11). The ordinate represents scattering response per unit volume, and the abscissa is the mean particle diameter. It is noted that a perfect response function would be indicated by a horizontal line. Since, in practice, mean diameters are on the order of 5 μm, it is evident that the slope of theoretical response deviates significantly from the idealized case. However, the response function can be compensated to approximate the ideal function. To this effect, an empirical algorithm

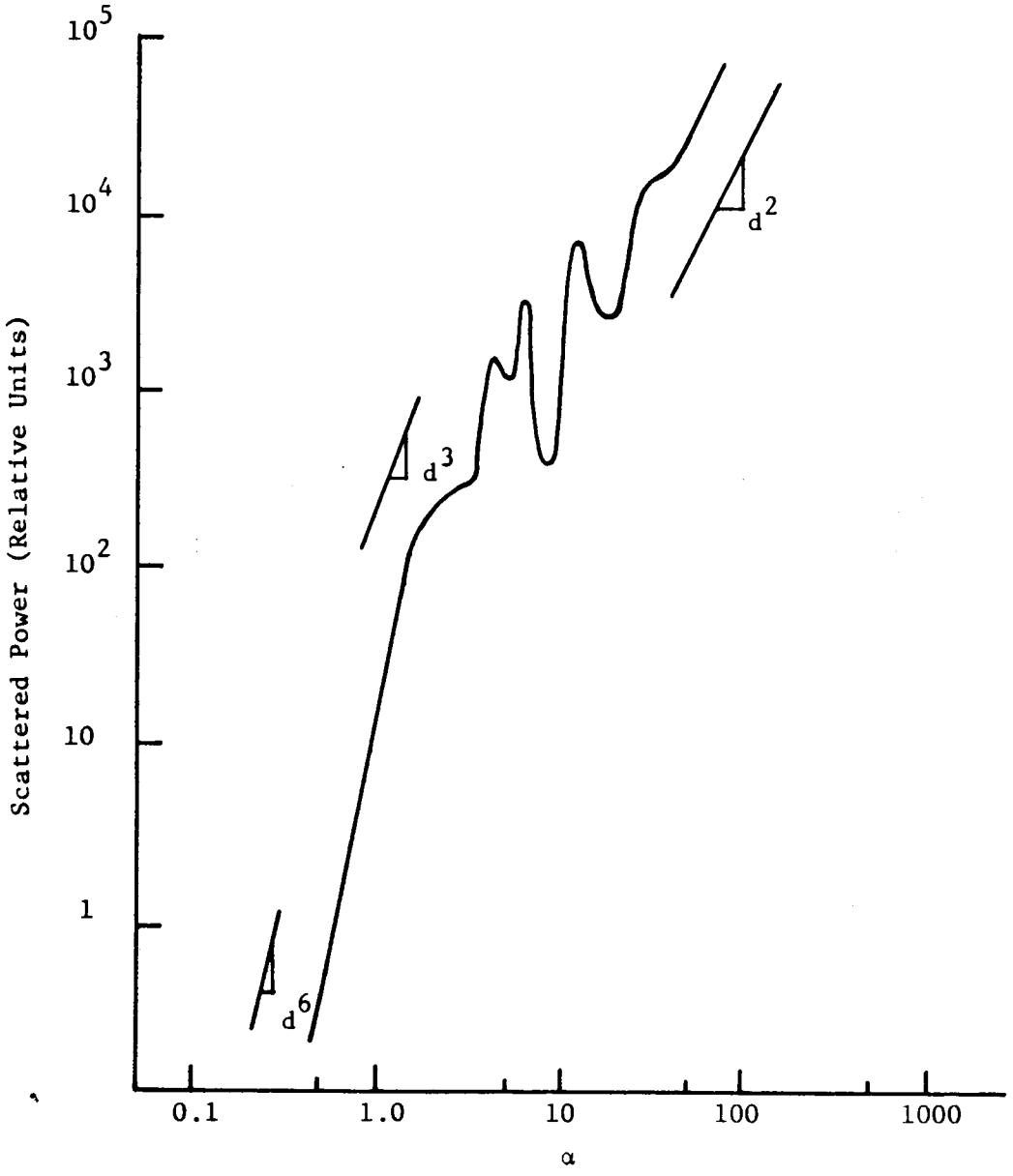


Figure 2-2. Forward scattered power vs. α.

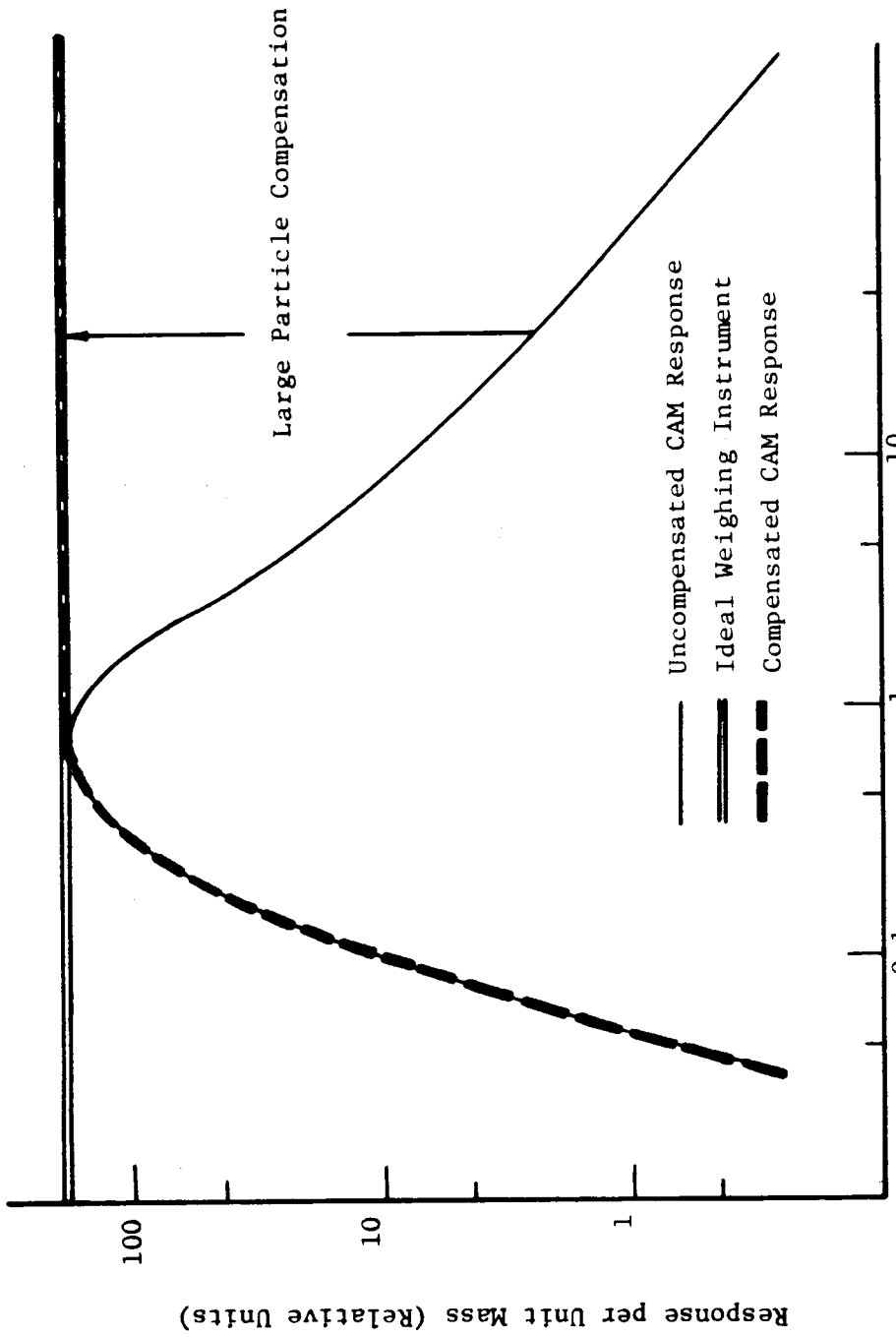


Figure 2-3. Response per unit mass vs. $\bar{d}_m$ mass mean diameter for CAM with large particle compensation.

is implemented in the microprocessor which essentially corrects the scattering response to the ideal case. This correction is indicated graphically in Figure 2-3 by the horizontal dashed line.

As a numerical example of the magnitude of uncompensated response error, consider a hypothetical distribution of spherical particles. Assuming a monodisperse distribution of 1 μm diameter particles with mass density (ρ) of 1.5 g/cm^3, the mass (m) of a single particle is given by:

$$\begin{aligned} m &= \frac{\pi}{6} d^3 \\ &= (1.5 \frac{g}{cm^3}) \frac{\pi}{6} (10^{-4} cm)^3 \\ &= 0.785 \text{ picograms} \end{aligned} \tag{2-2}$$

Now assume that 1,000 of these 1 μm particles are present in a sampling volume (V_s) of 1 cm^3. The mass concentration is given by:

$$\begin{aligned} \chi &= \frac{n \frac{\pi}{6} d^3}{V_s} \\ &= \frac{(1000)(7.85 \times 10^{-7} \mu g)}{(1 \text{ cm}^3)(10^{-6} \text{ m}^3/\text{cm}^3)} \\ &= 785 \ \mu g/m^3 \end{aligned} \tag{2-3}$$

In contrast, it is easily shown that a single 10 μm particle present in the sampling volume gives the same value of χ. Thus, for perfect mass concentration response function, it is seen that a 10 μm particle should scatter 1,000 times more radiation than a single 1 μm particle.

Inspection of Figure 2-3 shows that the ratio of scattering response for 10 μm and 1 μm spheres is more on the order of 100.

Therefore, if the detector electronics are calibrated to produce 785 mV for the 1 μm distribution, the 10 μm distribution, which ideally should yield the same output voltage, would give only $\frac{100}{1000}$ (785 mV) = 78.5 mV. This simplified example illustrates the need for some form of large particle compensation.

From this discussion, it is obvious that an uncompensated electro-optical detector cannot be expected to give accurate measurements of χ on widely varying size distributions. In particular, it is seen that the d^2 relationship for large particles causes an underweighing of particle mass.

In operation, the CAM System is programmed to compute a running average of the background level due to small particles. This data is stored digitally in the microprocessor and is representative of small particle mass. When a large pulse occurs, its peak value is compared with the background level, and if the difference is significantly larger than normal process variation, it is stored separately from the small particle data. In addition, the large particle data is input to a nine-channel pulse height analyzer (PHA), giving a voltage distribution that is approximately related to the large particle size distribution. An empirical compensation algorithm operates on the large particle data to correct underweighing errors. The total mass concentration is given by the sum of small particle data and compensated large particle data.

The purpose of the research was to explicitly calibrate the large particle response of the CAM System and to gain insight into the problems associated with electro-optical weighing of particulate mass. The basic approach was to compare simultaneously acquired cotton dust data provided by the CAM PHA and optical microscopy. The experimental methods are described in the next chapter and results are given in Chapter IV.

CHAPTER III

EXPERIMENTAL METHODS

Microscopic Analysis

In order to obtain accurate size distribution information for small particles, microscopic analysis is absolutely necessary. With cotton dust, where vastly different types of particulates are encountered, a qualitative as well as quantitative description of size is required. For very large particles, it is known that the scattered radiation is proportional to d^2 or the projected area of the particle. For irregular, nonsymmetrical particles, a relationship between volume and projected area must be found experimentally in order to calculate mass. Since it is assumed that the CAM responds linearly with area for large particles, the behavior of the V/A ratio will in effect define the mathematical form of the compensation algorithm. A calibration of the CAM System is achieved by correlation of the actual size distribution derived by microscopy with simultaneous PHA count distribution from the CAM System. This correlation should provide insight into the collection efficiency of the CAM as well as the fractional efficiency of the vertical elutriator.

The CAM experimental prototype is designed so that the dust-laden air flows directly through the optically defined sampling volume and into a standard 37 mm filter holder identical to the cassettes used with the Lumsden-Lynch vertical elutriator. A Millipore^R membrane filter is enclosed in the cassette so that the particles are deposited on the porous filter surface as air flows out of the CAM. With this arrangement, the filter samples can be removed and analyzed either gravimetrically

or microscopically and correlated with corresponding CAM data. For microscopic analysis, the exposed filter cassettes are carefully removed from the CAM sensor, sealed, and transported to a clean laboratory where the samples are prepared for microscopic examination.

Both light microscopy and electron microscopy are commonly used in particulate size analysis. Each method has its advantages and choice depends primarily on application. In this study, optical microscopy with transmitted illumination was utilized. Although much greater resolution and depth of field can be achieved using the scanning electron microscope, the entire filter cannot be mounted on one specimen stud, and so the sample must be sectioned and viewed separately (12). This situation is clearly undesirable since a large portion of the filter must be viewed in order to obtain a statistically valid number of large, rare particles. Also this procedure requires excessive handling of the sample which might disturb the particle distribution and yield erroneous results. In addition, it was observed that the porous filter membrane structure itself obscured many of the smaller particles, making observation difficult. Finally, user time is very expensive in comparison to standard light microscopy.

A Zeiss Universal Research Microscope was utilized for all particle size analysis. Essential to all microscopic size analysis are several microscope features (13,14):

1. Mechanical X-Y stage with graduated verniers.
2. High quality objective lens.
3. Eyepiece reticle.
4. Good source of illumination.
5. Calibration standard.

The research microscope was equipped with a circular mechanical stage with 50 X 75 mm range and accuracy of .1 mm using the X-Y verniers. A 10X eyepiece with 10 mm linear graduated scale graticule was used to size individual particles directly. The microscope was adaptable to either transmitted or incident illumination, but poor contrast was observed using incident illumination. In order to utilize transmitted illumination, a special procedure was required to prepare the microscopic sample.

The porous structure of the plastic Millipore filter gives the surface an opague pigment when viewed under the microscope. However, the filter substrate can be rendered transparent by melting, which fills all the air spaces in the membrane, causing a uniform refractive index. In addition, when the dissolved filter hardens, the entrained particles become bonded to the filter surface leaving a conveient permanent specimen, suitable for examination using transmitted illumination. A solution of equal parts of hexane, paradioxane, and 1,2-dichlorethane was used to melt the plastic membrane filter on a clean, glass microscope slide (15). The contaminated filter is wetted with this solution and then exposed to acetone vapor which hardens the filter and bonds it to the glass slide. Using this simple procedure, specimens could be mounted easily and labelled for future reference.

The Zeiss Universal Microscope was equipped with two achromatic objective lens with magnifications of 10X and 40X. With the high power objective, the overall magnification was calculated to be 800X or 1.20 μm/div as measured on the eyepiece reticle. As a cross-check, known calibration standards were sized, and overall magnification was

measured. Using Dow Diagnostics Uniform polystyrene spheres, samples of three different size particles were prepared and viewed at 800X. The mean sphere diameters were 0.5 μm, 1.101 μm, and 5.7 μm, with standard deviations of 0.0027 μm, 0.0055 μm, and 1.500 μm, respectively. The average measured magnification was in good agreement with the nominal value. A similar calibration was performed on the 10X objective, using a 100 μm stage micrometer.

In order to obtain a representative sample of the entire mass distribution across the filter, special methods of determining the locations of sample points were required. Bethea and Morey utilized a random sampling procedure in obtaining particle statistics (16). Without making too many assumptions, a sampling procedure that is mathematically and statistically well founded was devised and employed in all microscopic analysis.

Equal Area Sampling

Assume that some given mass distribution m(r) exists along an arbitrary diameter of a disk of radius R. Assuming that the mass distribution function is symmetrical about the axis of revolution, the entire mass M can be found using the method of cylindrical shells. This problem is entirely analogous to finding the volume of a solid of revolution. From elementary calculus, the volume generated by rotating a plane area defined by some function $y = f(x)$ is given by:

$$V = 2\pi \int_a^b x\, f(x)dx. \qquad (3\text{-}1)$$

If the m(r) is the incremental mass distribution along one radius of a disc, the entire mass M across the disc is found by integration:

$$M_{TOT} = 2\pi \int_{o}^{R} rm(r)dr. \tag{3-2}$$

If m(r) = 0 for r > R, the total mass M_{TOT} is proportional to the mean value of the incremental mass distribution $\bar{m}$. When the incremental mass distribution m(r) is not given in explicit terms as a continuous function, the required exact integration is not possible. Instead, the experimentally obtained data may be used in a curve fitting procedure to approximate m(r).

Discrete data are often plotted in the form of a histogram or bar graph. By spacing the histogram cells symmetrically about the sample points, a piecewise continuous curve approximating the actual distribution is obtained. Although the shape of the actual distribution function is distorted, integration yields acceptable results. When the histogram represents an incremental mass distribution function m(r), the total mass along a radius r is found simply by summing the areas of the histogram cells. For the i^{th} cell, the incremental mass is given by:

$$\Delta m_i = m(r_i)\Delta r_i \tag{3-3}$$

Where $m(r_i)$ is the value of the mass distribution at the midpoint of the cell r_i, and Δr_i is the width of the i^{th} cell, the total incremental mass along one radius is found by integration:

$$M_{TOT} = \int_{o}^{R} m(r)dr \simeq \sum_{i=1}^{N} m(r_i)\Delta r_i \tag{3-4}$$

where N is the number of sample points along the radius. Thus, the total mass across the disc is:

$$M_{TOT} = 2\pi \int_{o}^{R} rm(r)dr \simeq 2\pi \sum_{i=1}^{N} r_i m(r_i)\Delta r_i . \tag{3-5}$$

Note that if the term $r_i \Delta r_i$ is made to be constant, the approximate total mass is found by summing the N values of the incremental mass distribution function $m(r_i)$ and multiplying by the appropriate scale factor. It is easily shown that an annulus of inner radius $r - \frac{\Delta r}{2}$ and outer radius $r + \frac{\Delta r}{2}$ bounds an area given exactly by

$$A = 2\pi r \Delta r. \tag{3-6}$$

Therefore, when r_i and Δr_i are chosen so that each histogram cell represents an equal area around the entire disc, the total mass is:

$$M_{TOT} = \sum_{i=1}^{N} A_i m(r_i) = A_{TOT} \sum_{i=1}^{N} m(r_i) \tag{3-7}$$

where A_i is the area of each annulus.

The boundaries of each histogram cell are determined by the number of sample points along one radius. If the disc is divided into N sample zones, the area of each zone must be $A_i = \frac{\pi R^2}{N}$. The zone boundaries Z_i are then successively computed using the relation:

$$A_i = \pi (Z_i^2 - Z_{i-1}^2) \tag{3-8}$$

noting that $Z_i = r_i + \frac{\Delta r_i}{2}$ and $Z_{i-1} = r_i - \frac{\Delta r_i}{2}$, as shown in Figure 3-1.

By choosing the location of the sample points in such a way, a representative radial mass distribution may be obtained by sampling along a single radius. The results are independent of the shape of the distribution function m(r) and only rely on the assumption of radial symmetry. For arbitrary distribution functions, random selection of sample points is only valid when a large number of data points are obtained. Equal area sampling assures that each data point is weighted equally, without requiring an excessively large data base.

The required number of sample points is determined by the particle density across the filter surface. For counting statistics the confidence level of the microscopic analysis is a function of the number of particles counted in a certain size class. Tests of significance show that in general the standard error of determination is inversely proportional to the square root of the number of sample (17,18).

Data Interpretation

In order to obtain a sufficient data base over the entire range of particle sizes, three separate examinations were performed on each filter sample. For the smallest particles measured, approximately less than 15 μm in diameter, equal area sampling was utilized at a magnification of 800X. Using a linear 10 mm eyepiece graticle with a 0.1 mm graduation, the width of the viewing area was determined to be 120 μm. The sampling area was defined by revolving the eyepiece 180 degrees and counting particles within the enclosed circle. At 800X, the sampling area is calculated to be 1.13×10^{-2} mm^2 or 1.05×10^{-3}% of the entire

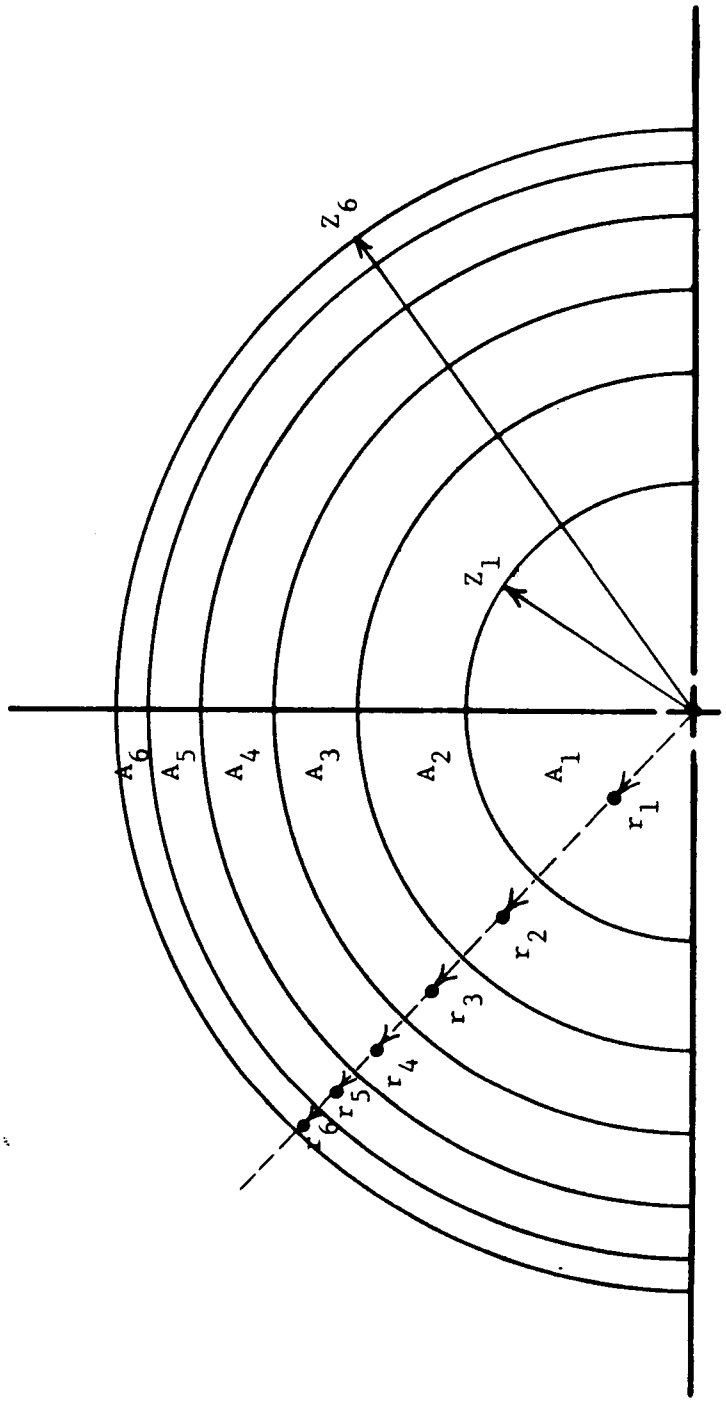


Figure 3-1. Filter sections for equal area sampling.

filter area. Upon determination of the number of sample points to be observed along one radius, the sample locations r_i were calculated and positioned successively using the graduated stage verniers. At each sample point, all particles within the defined field of view were measured in two perpendicular dimensions and grouped by arbitrary size classes. Since cotton dust particles are not strictly spherical, the longest linear dimension d_M and the perpendicular minor dimension d_m are both measured in order to calculate an approximate size and shape. An elliptical shape factor was chosen to calculate particle area and volume since the majority of dust particles were observed to have rounded edges. An advantage of using an ellipse as the assumed shape is that the equations for area and volume reduce to the spherical case when $d_M = d_m$.

After each traverse was completed, the volume and projected area associated with each particle is computed and tabulated. For an ellipsoid of revolution, the projected area and volume are given by

$$A = \frac{\pi}{4} d_M d_m \tag{3-9}$$

and

$$V = \frac{\pi}{6} d_M d_m^2. \tag{3-10}$$

Since the CAM is assumed to respond to area for large particles, it is logical to group the sampled particles by their respective projected areas. Due to the wide range of particle size encountered,

it is convenient to plot their frequency distribution using a logarithmic size axis. Spacing the class boundaries in a geometric progression, the area of each histogram cell may be interpreted as being proportional to the number of particles within the class interval. By classifying particle size by projected area, the ambiguous nature of defining equivalent diameter spheres is avoided.

The large particle content ($\tilde{>}$ 15 μm diameter) is determined by performing a second traverse at the lower magnification 200X. The field of view at 200X is approximately 480 μm in diameter or .0168% of the entire filter area. Utilizing equal area sampling, the upper portion of the mass distribution is determined as before. Where the two determinations overlap, 5 μm $\tilde{\leq}$ d_{eq} $\tilde{<}$ 15 μm, the results are averaged to smooth statistical fluctuations. The average mass in the overlapping size classes is determined by number weighting. The average mass of the i^{th} cell is calculated as:

$$m_i^* = \frac{(n_i m_i)\big|_{200X} + (n_i m_i)\big|_{800X}}{n_i\big|_{200X} + n_i\big|_{800X}}. \qquad (3\text{-}11)$$

It was found that the giant particles ($\tilde{>}$ 25 μm) are extremely rare and equal area sampling proved to be inadequate without a large number of sample fields. For accurate statistics, the entire filter was scanned, and only the very largest particles were counted. Although few in number, the giant particulates can have a significant effect upon the mass distribution.

Compounding the problem is the presence of large elongated fibers which make volume calculations difficult. Definitely not elliptical in shape, the fibers were treated as long solid cylinders with unknown mass density. It is known that cotton fibers are actually hollow cylinders with a mass density comparable to that of cotton dust. Therefore, the main problem in determining fiber mass is in the measurement of wall thickness. As a numerical example, a hollow 15 μm diameter fiber with 2.5 μm thick walls contains about 56% as much volume as a solid cylinder of equal outside dimensions. For simplicity, it was decided to consider the fiber distribution separately from the dust particle mass distribution.

The particle mass distribution was determined by tabulating the results of microscopy in the form of Table 3-1. The three size categories refer to the different sampling techniques utilized. The particles are grouped by projected area A_i, where the entry represents the lower boundary of the size class. For example, the row labeled 16 μm^2 includes all particles with projected areas greater than or equal to 16 μm^2 but less than 32 μm^2. The equivalent diameter d_{eq} is defined as the diameter of a sphere of equal projected area A_i.

The number of particles counted in equal area sampling is denoted n_i, and the total number extrapolated to the whole filter is N_i. The total number of particles in one size class N_i is related to the number sampled n_i through the ratio of total filter area to total sampled area. The total volume in each size class is found by summing the volume of each particle counted and normalizing by the same proportionality constant. The mass m_i is proportional to the volume by the density of

Table 3-1. Microscopy summary sheet.

		Small Particles			Large Particles			Giant Particles		
A_i	d_{eq}	n_i	N_i	m_i	n_i	N_i	m_i	N_i	m_i	m_i*
(μm^2)	(μm)			(μg)			(μg)		(μg)	(μg)
1	1.13	61	289,933	0.394						0.394
2	1.6	35	166,355	0.577						0.577
4	2.3	52	247,156	2.263						2.263
8	3.2	15	71,295	2.863						2.863
16	4.5	4	19,012	1.405	53	15,746	1.361			1.365
32	6.4	3	14,259	2.578	25	7,427	1.121			1.277
64	9.0	2	9,506	6.954	11	3,268	2.401			3.101
128	12.8	1	4,903		3	891	1.729			1.729
256	18.0				1	297	1.032	160	1.19	1.19
512	25.5							42	0.754	0.754
1,024	36.1							22	1.002	1.002
2,048	51							6	0.796	0.796
4,096	72.2							2	0.377	0.377
8,192	102.1									

M_P = 15.596 μg

(M_T = 18.082 μg)

cotton dust, approximately 1.5 g/cc. The results of each determination are collected and averaged in the last column labeled m_i^* which is representative of the particle mass distribution. The total mass of particles M_p is found by simply summing the values of m_i^*.

The total mass including fibers M_T is calculated from the CAM algorithm which is known to approximate VE measurements. The difference in total mass and particle mass is assigned to fibrous content and is designated M_f. Very small particles ($\tilde{<}$ 1 μ) are known to have little effect on the mass distribution, typically less than 1% of the total mass and therefore are neglected in the analysis.

The problem of calculation of fiber mass and projected area must necessarily be treated separately from particle computations. Several assumptions must be made in order to obtain a reasonable approximation of the mass distribution. Since by definition, fibers are extremely elongated ($d_M \tilde{>} 5\ d_m$), the orientation of the fiber as it passes through the beam has a significant effect upon the projected area or shadow area that is presented to the optical sensor.

Fiber Orientation

Sedimentation studies have shown that fiber orientation is related to flow characteristics and corresponding Reynolds number (19). For the transitional flow regime, between laminar and turbulent flow, it is believed that the fiber remains in the initial orientation as it gravitates downward. The fiber assumes a horizontal position in laminar flow and randomly tumbles in turbulent flow. Although the vertical elutriator is designed for laminar flow, its characteristics are not well characterized.

Assuming a random orientation as the fiber passes through the optically defined sampling volume, an average value of projected area can be computed. The geometry of Figure 3-2 is used in conjunction with basic probability theory to compute the mean projected area of an arbitrary fiber of length d_M and diameter d_m. In Figure 3-2, the Z-axis represents the optical axis and the X-axis is the direction of motion. The longitude and co-latitude, θ and ϕ, respectively, are assumed to be uniformly distributed on $(0, \pi/2)$. For $\phi = \pi/2$, the fiber is perpendicular to the optical axis and the maximum projected area is presented. The minimum projected area results when the fiber is in line with the optical axis or $\phi = 0$. Note that a single octant is sufficient to describe the projected area of all possible orientations. The joint probability density function is given by:

$$p(\theta,\phi) = \frac{4}{\pi^2} \qquad \begin{cases} 0 < \theta \leq \frac{\pi}{2} \\ 0 < \phi \leq \frac{\pi}{2}. \end{cases} \tag{3-12}$$

It is easily shown that the projected length ℓ is a function of ϕ only:

$$\ell(\theta,\phi) = d_M \sin\phi. \tag{3-13}$$

The mean projected length ℓ is found by computing the expected value of $\ell(\theta,\phi)$:

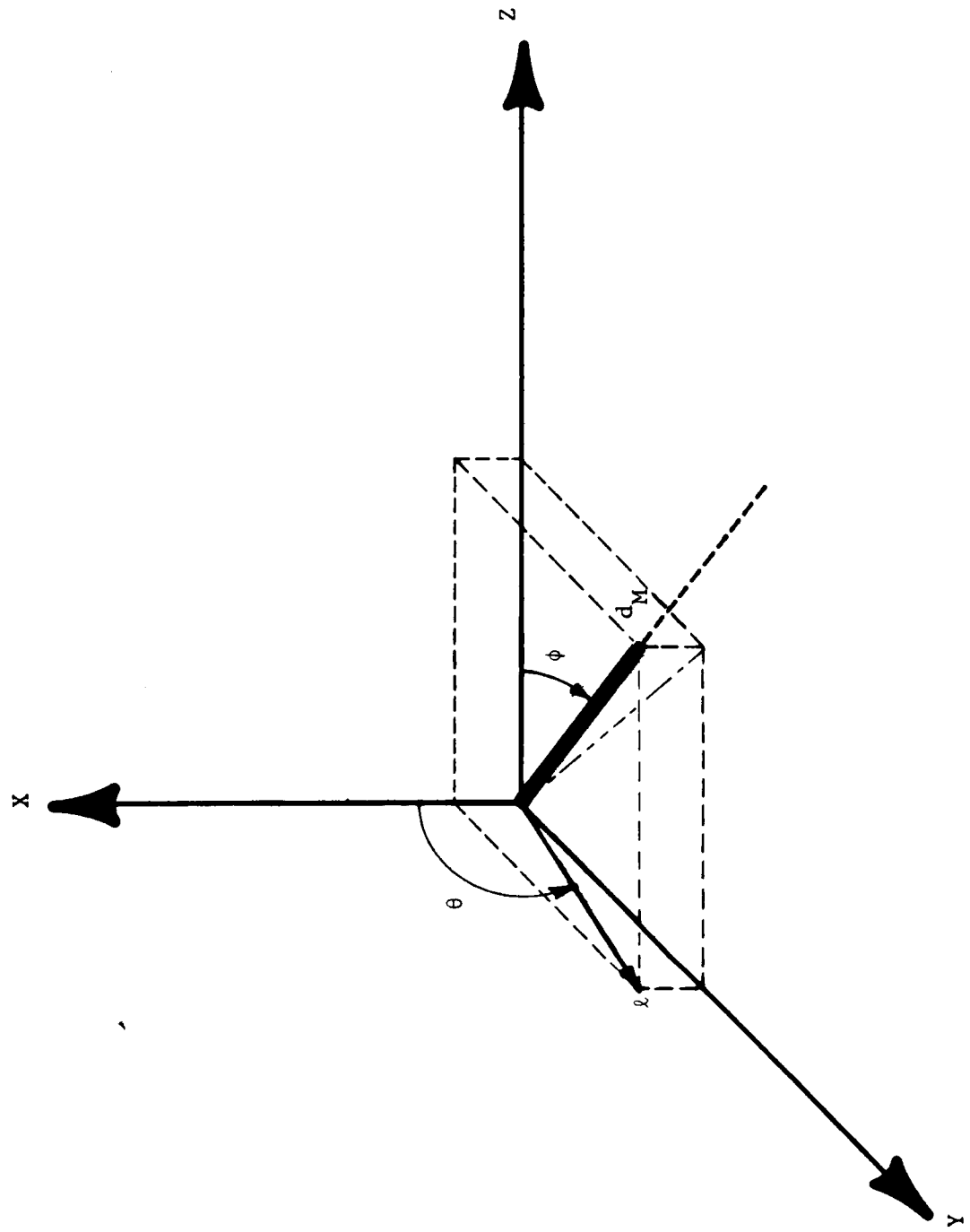


Figure 3-2. Fiber orientation geometry.

$$E[\ell(\theta,\phi)] = \bar{\ell} = \int_{-\infty}^{\infty}\int_{-\infty}^{\infty} \ell(\theta,\phi)p(\theta,\phi)d\theta d\phi$$

$$= \frac{4d_M}{\pi^2}\int_0^{\pi/2}\int_0^{\pi/2} \sin\phi d\theta d\phi$$

$$= \frac{2}{\pi}d_M. \qquad (3\text{-}14)$$

Thus, the mean projected length is about 65% of the actual length. For a horizontal fiber $\theta = \pi/2$ and the expected value is:

$$E[\ell(\phi)] = \frac{2}{\pi}d_M\int_0^{\pi/2}\sin\phi d\phi = \frac{2}{\pi}d_M. \qquad (3\text{-}15)$$

Assuming that d_M is much larger than the diameter d_m, the mean projected area is proportional to $\bar{\ell}$, whether the flow is laminar or transitional. Since, in general, fibers settle on the filter surface in their plane of maximum stability, the maximum projected area is seen through the microscope. The mean projected area is found by scaling by the factor of $2/\pi$.

Relationship between Stokes Diameter and Projected Diameter

The aerodynamic behavior of long cylindrical particles has been studied extensively, and numerous empirical models exist (20). One popular method of determining fiber flow characteristics is found in defining equivalent diameter spheres. Empirical equations have been determined which relate geometrical properties of solid rods to an equivalent Stokes diameter sphere. Stokes' law may then be applied and the terminal settling velocity of the fiber determined. A long cylindrical fiber moving perpendicular to its major axis has an

equivalent Stokes diameter approximated by:

$$d_{s_\perp} \cong \frac{4d_m\beta}{3(\ln(2\beta) + 1/2)}, \tag{3-16}$$

where d_m is the minor axis diameter, and β is the aspect ratio $\frac{d_M}{d_m}$. For a fiber moving parallel to its major axis d_s is given by:

$$d_{s_{\parallel}} = \frac{2d_m\beta}{3(\ln(2\beta) - 1/2)}. \tag{3-17}$$

These two equations set the limits on the Stokes diameter of a randomly oriented fiber. For a fiber perpendicular to the optical axis, the maximum projected diameter is:

$$d_{eq_{Max}} = \sqrt{d_M d_m} = \sqrt{\beta d_m^2} = d_m\sqrt{\beta}. \tag{3-18}$$

The ratio of Stokes diameter to the maximum projected diameter for a long horizontal fiber is calculated to be:

$$\frac{d_{s_\perp}}{d_{eq_{Max}}} = \frac{4\sqrt{\beta}}{3(\ln(2\beta) + 1/2)}. \tag{3-19}$$

For a vertical fiber, the ratio $\frac{d_{s_{\parallel}}}{d_{eq_{Max}}}$ is given by:

$$\frac{d_{s_{\parallel}}}{d_{eq_{Max}}} = \frac{2\sqrt{\beta}}{3(\ln(2\beta) - 1/2)}. \tag{3-20}$$

The two cases are plotted in Figure 3-3, where the curves represent the minimum values of the ratio. If the average value is taken along the center of the bounded region, it is seen that the Stokes diameter is greater than the projected diameter for all values of $\beta \tilde{>} 10$. It should be noted that the approximate Stokes diameter equations are based on the assumption of unit density and large aspect ratios. However, since the fibers are known to contain voids, the assumed bulk density of 1 g/cm^3 is probably more accurate than the true mass density of 1.5 g/cm^3.

The variable nature of fiber cross-sectional geometry requires empirical methods of determining fiber volume by microscopic examination. However, since the approximate fiber mass can be estimated using the CAM algorithm, the average fiber volume can be deduced. From microscopy, the total mass in compact particles M_p is determined using the bulk density of 1.5 g/cc. The difference in total mass predicted by CAM and the mass in compact particles gives the approximate mass of large fibers. Thus, assuming that the fiber is a solid cylinder, a normalized value of fiber mass density is computed that gives the total mass predicted by CAM. This artificial value of mass density is given by the ratio of total fiber mass to the total fiber solid volume. It was found that, in general, this solid volume mass density is on the order of 50% of the true mass density. Using a value of about .75 g/cc, individual fiber mass is computed from fiber solid volume, and the results are added to the particle distribution, giving the overall mass distribution.

It is seen that, on the average, the actual fiber volume is roughly half the solid volume computed from the outside dimensions.

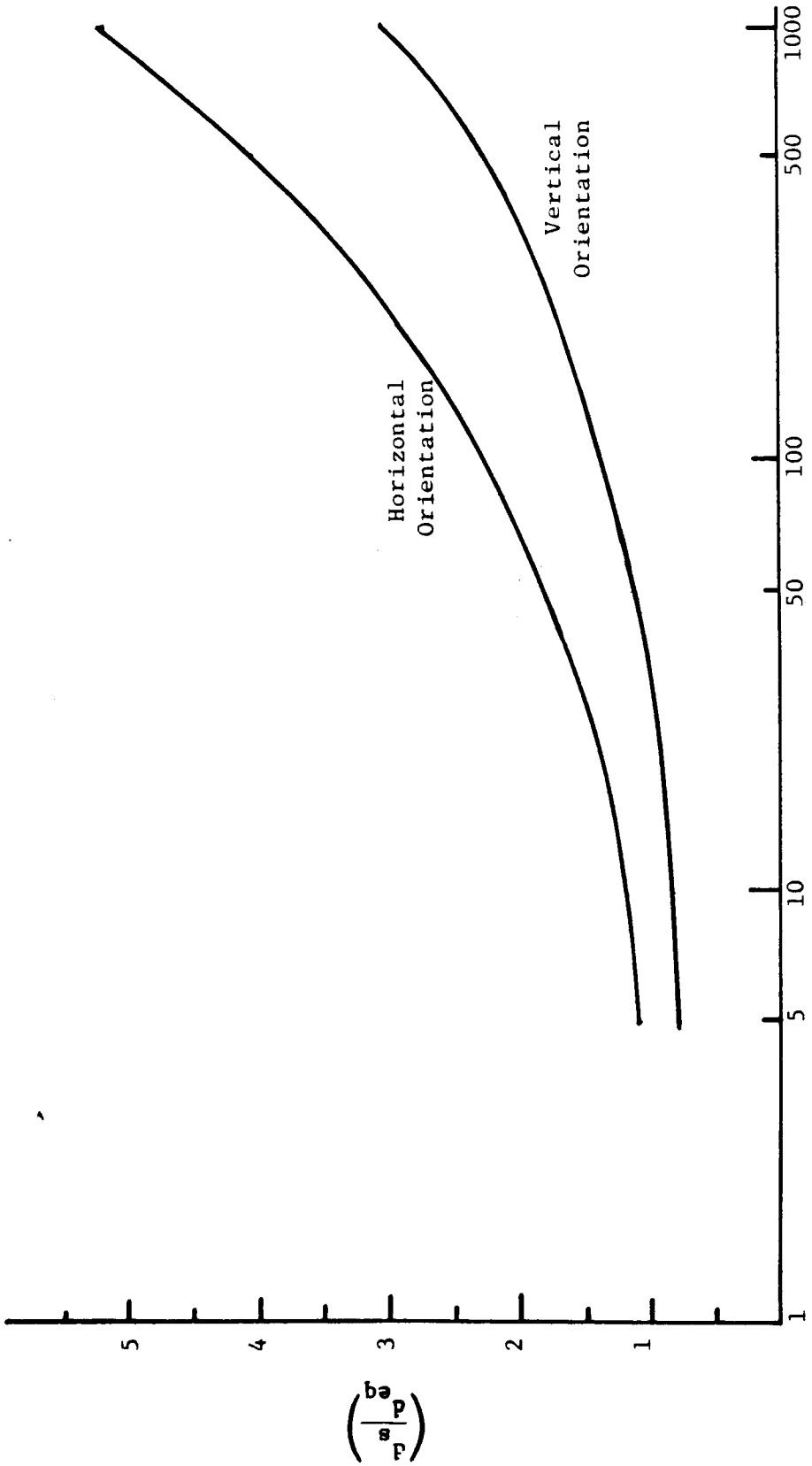


Figure 3-3. Ratio of Stokes diameter to projected diameter vs. aspect ratio, β.

This fact implies that the actual cross-sectional area is about 50% of the area enclosed by the outer diameter. Detailed fiber geometry studies utilizing electron microscopy have shown that typical mature cotton fibers have outer diameters of about 15 μm and wall thickness on the order of 2.5 μm, giving cross-sectional area ratios of 56% (21). Thus, the experimentally determined ratio based on fiber mass agrees with measured values obtained using electron microscopy.

CHAPTER IV

EXPERIMENTAL RESULTS

Overview

A common approach to calibrating aerosol detectors is to supply monodisperse particles of known size to them and then evaluate the resulting response. This does not apply well to cotton dust, which is a heterogeneous mixture of various particle sizes, shapes, and compositions, and with these parameters varying from process to process. It was decided that more realistic results could be obtained using actual mill data.

As explained in Chapter II, the CAM sensor produces distinguishable pulses, for large particles, over the quasi-DC background. These pulses are randomly sampled in time. It is important to realize that the CAM pulse height histogram must be interpreted as an average response to individual particle classes.

Still further, for irregularly shaped particles, such as fibers, which presumably are randomly oriented in the weighing volume, the interpretation of the pulse height histogram must similarly be in an average sense.

The calibration experiments compare the CAM pulse height histogram with simultaneously acquired optical microscopy data. For emphasis, the CAM sensor "saw" the same particles later characterized microscopically. For further emphasis, all data are from typical cotton manufacturing processes.

Thus, the simultaneous microscopy data became real-world calibration particles with which to compare the CAM pulse height distribution. This is contrasted with laboratory calibration with known, and perhaps unrealistic, particles.

Two fundamentally different experimental approaches were taken. One involved calibration on the basis of penetration efficiency and the second used an altogether different differential, large particle mass determination. The former proves that the pulse height distribution responds directly to average projected area. The latter generates an explicit calibration for large particle contributions, fractionally, to total mass but is sensitively dependent on the implicitly determined total mass algorithm established through extensive side-by-side testing with the reference gravimetric method. It follows that the calibration results are fundamentally different in their interpretation.

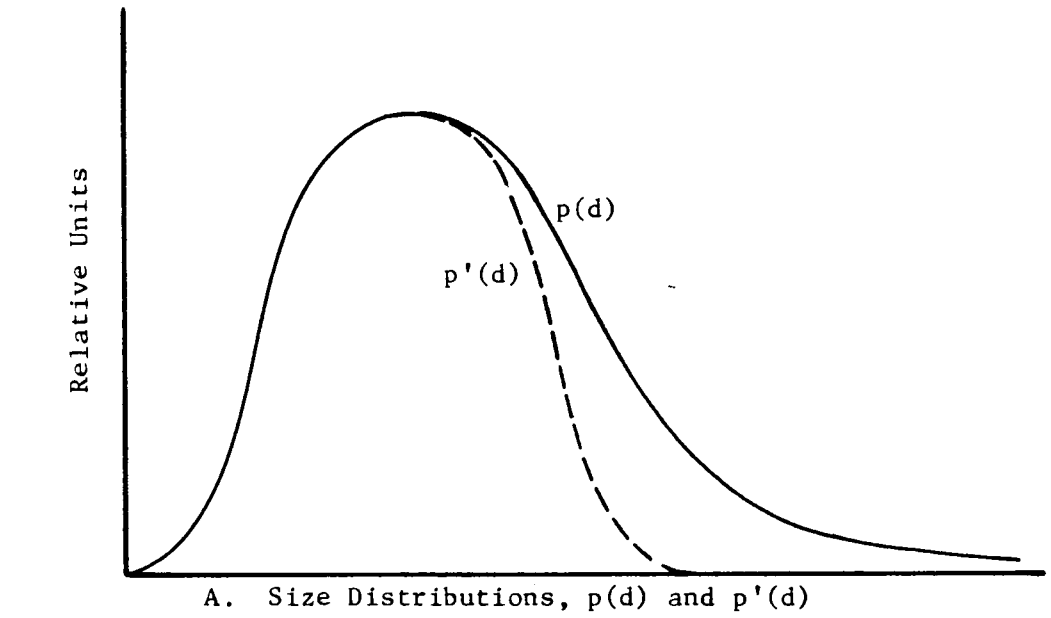
Penetration Efficiency Calibration

This method has several analogous features to determination of linear system transfer functions. Instead of working with known absolute numbers, an equally viable method of correlating input-output data is found in differential techniques. In the "dynamic" approach, some perturbation is applied to the input, and the resulting change in the output signal may be correlated regardless of the initial "static" condition or absolute numbers representative of it. Thus, if the particle distribution is thought of as the input signal and the CAM voltage distribution as the output signal, some arbitrary perturbation imposed upon the particle distribution results in an output change

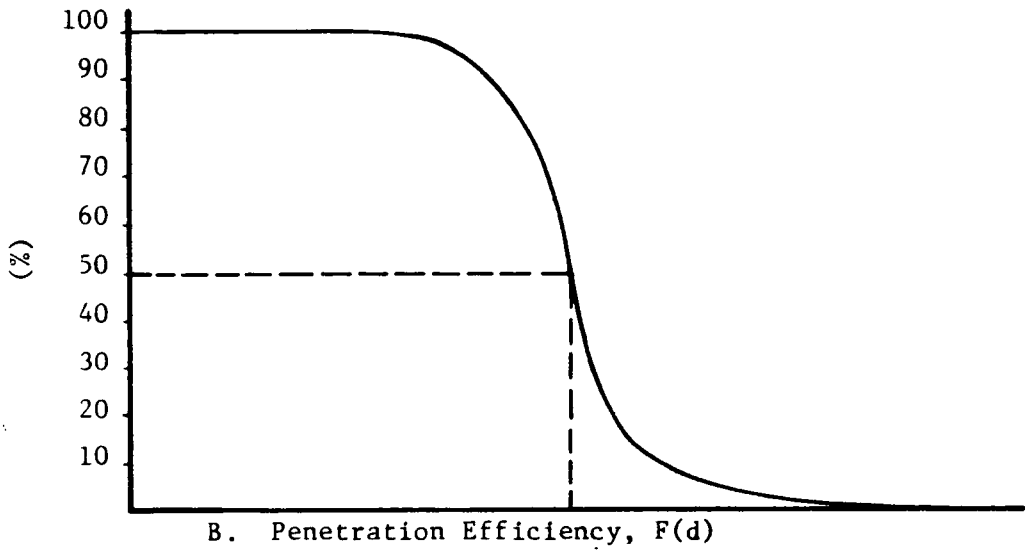
which is indicative of the system transfer function.

In communication theory, system responses are often determined by passing filtered random noise through the system under study and mathematically manipulating the resulting output power spectral density. In the analogous mechanical system, the random variable is particle size, and the filtering effect may be obtained by passing the initial particle distribution through some sort of sieve or fractional separator. If the process is stationary (time invariant), the filtered distribution may be expressed as a fraction of the original distribution, and the use of absolute numbers is avoided. This ratio will be termed the penetration efficiency F(d) of the filtering device and is assumed to be a function of particle size only. For a low-pass filter, F(d) will be a monotonically decreasing function. The value of d where F(d) = 0.5 is termed the aerodynamic cutoff diameter of the filtering device. In Figure 4-1, a typical probability density function p(d) and its corresponding filtered version p'(d) are plotted together on the upper graph. The resulting penetration efficiency curve F(d) is shown in the lower graph with the cutoff diameter $d_{50\%}$ indicated. The random variable d is not necessarily a spherical diameter but may be any size-related parameter of interest.

The output voltage distribution from the CAM System may be treated in an analogous manner, with the random variable being pulse voltage instead of particle size. The penetration efficiency curve derived from output data may then be correlated with the actual filter penetration efficiency curve. Using several different types of filter devices, a wide range of data points is obtained, and the approximate



A. Size Distributions, p(d) and p'(d)



B. Penetration Efficiency, F(d)

Figure 4-1. Typical p(d), p'(d), and F(d) curves.

system calibration is determined. The only restrictive assumption implied in this procedure is that the CAM System samples independently of grain loading or count rate.

It was found that nylon fabric provided a conveient sieve material for filtering the particle distribution. Inserted between the half-size vertical elutriator and the CAM sensor, a single layer of fabric proved to be a reliable filter with repeatable characteristics. Alternating between filtered and normal runs, the average penetration efficiency for each filter was determined. By averaging between adjacent runs, errors due to temporal variations in the mill environment are reduced.

Three different nylon filter materials were chosen on the basis of their respective filtering characteristics as determined in the mill from CAM PHA information. Each filtered run was immediately preceded and followed by a normal run so that an average ambient elutriated distribution was obtained. The microscopy histograms were then determined and the values of the penetration efficiency in each histogram cell were computed. A continuous curve is drawn through the data points located at the geometric means of each histogram cell. The three penetration efficiency curves are shown in Figure 4-2. Note that the particle projected area is represented along the logarithmic abscissa. The aerodynamic cutoff diameters for the three filters are calculated to be 6.13 μm, 8.77 μm, and 15.79 μm.

The corresponding CAM penetration efficiency curves are shown in Figure 4-3. The abscissa is representative of CAM output voltage on a logarithmic scale. The 50% cutoff points are seen to occur at output levels of 28.25, 68.6, and 294.1 mV. These values may be correlated

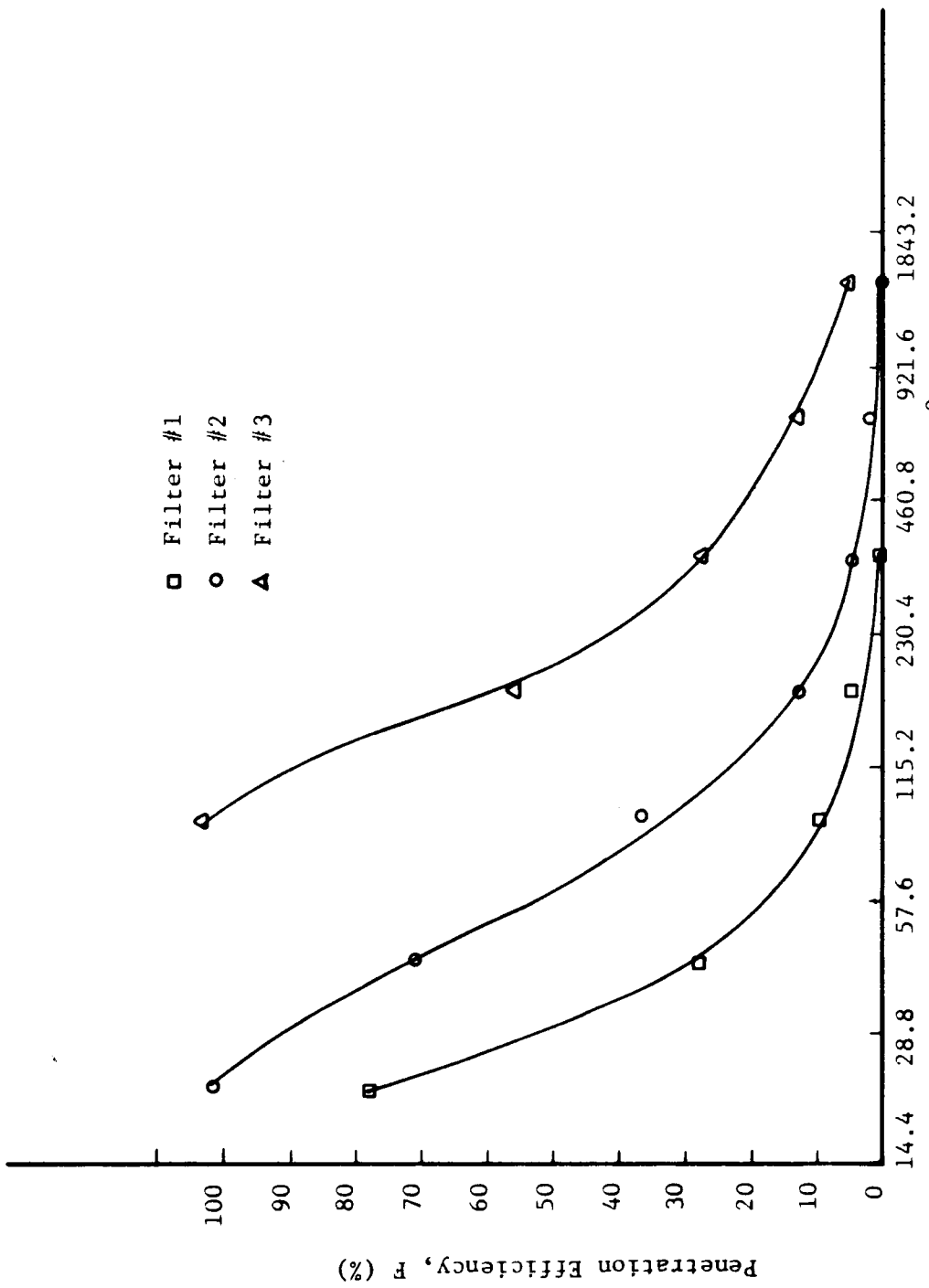


Figure 4-2. Penetration efficiency functions by optical microscopy.

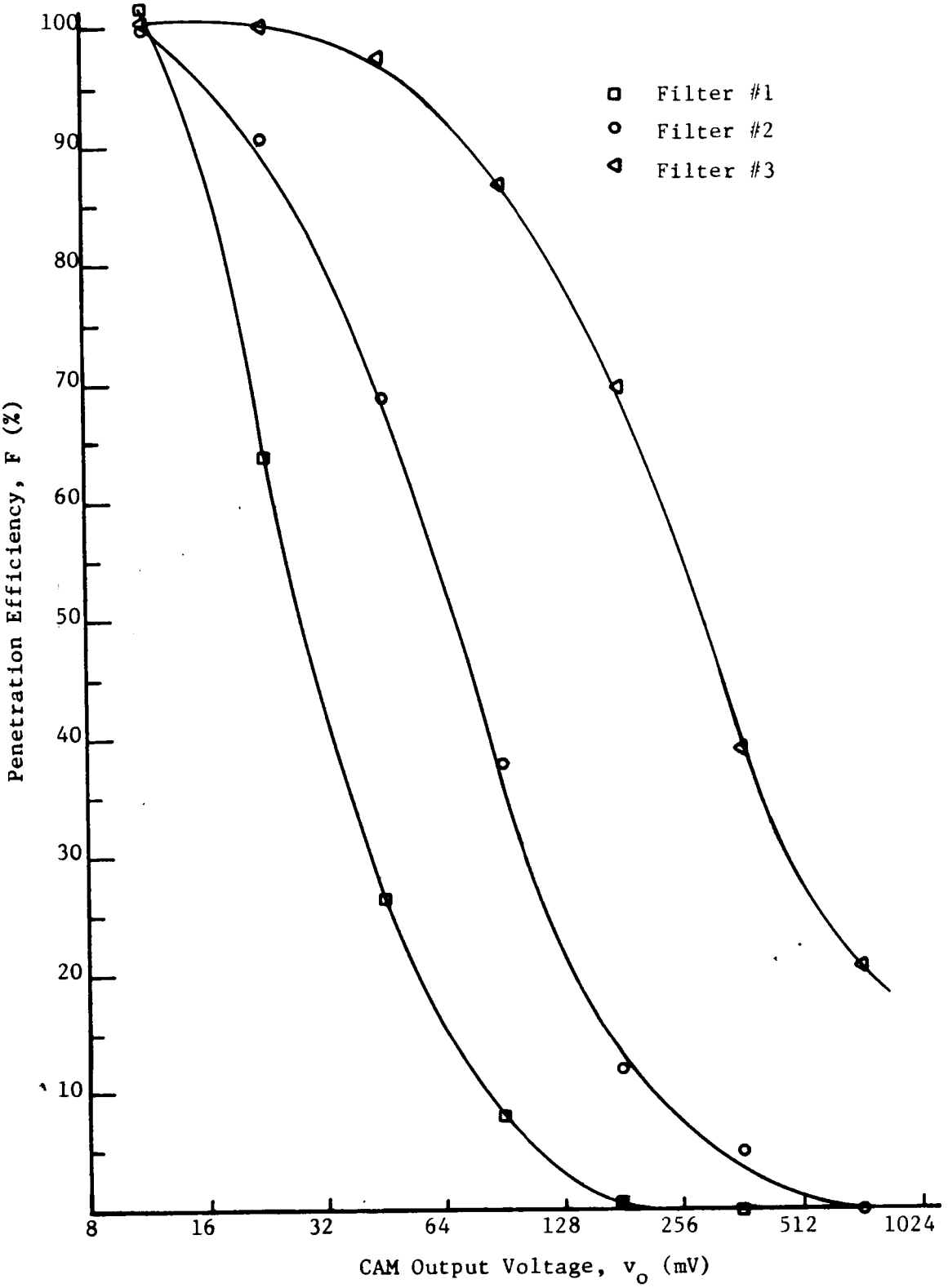


Figure 4-3. Penetration efficiency functions by CAM output data.

directly to the cutoff diameters determined above. By repeating this procedure at different levels of penetration efficiency, several data points are obtained, and system linearity may be checked. The calibration results are shown in Figure 4-4 with a linear function fitted to the data. An excellent fit is observed, particularly on the low end where there is very little scatter in the data. This is expected though, since the vast majority of these particles approximate spheres, and the associated projected area is independent of orientation. The theoretical slope may be drawn using the assumption that the scattering response is proportional to the projected area of the particle. If the particle projected area is doubled, the CAM output voltage should also increase by a factor of 2. From Figure 4-4, it is evident that the measured slope is within 5% of the theoretical case.

As a cross-check of the calibration results, the known theoretical characteristics of the vertical elutriator may be utilized. It has been shown theoretically that the vertical elutriator has an aerodynamic cutoff diameter of about 15 μm. From the initial calibration, it is apparent that the VE cutoff diameter should occur at an output voltage of about 225 mV. The predicted vertical elutriator penetration efficiency function was determined by running the CAM System with no preseparator, thereby giving the ambient distribution. The VE penetration efficiency was computed by forming the ratio of the elutriated distribution to the ambient distribution. Figure 4-5 shows the VE penetration efficiency function as predicted by the CAM System. It is seen that the aerodynamic cutoff diameter occurs at an output voltage of 128 mV. The calibration curve of Figure 4-4 implies an aerodynamic cutoff diameter of 11.8 μm,

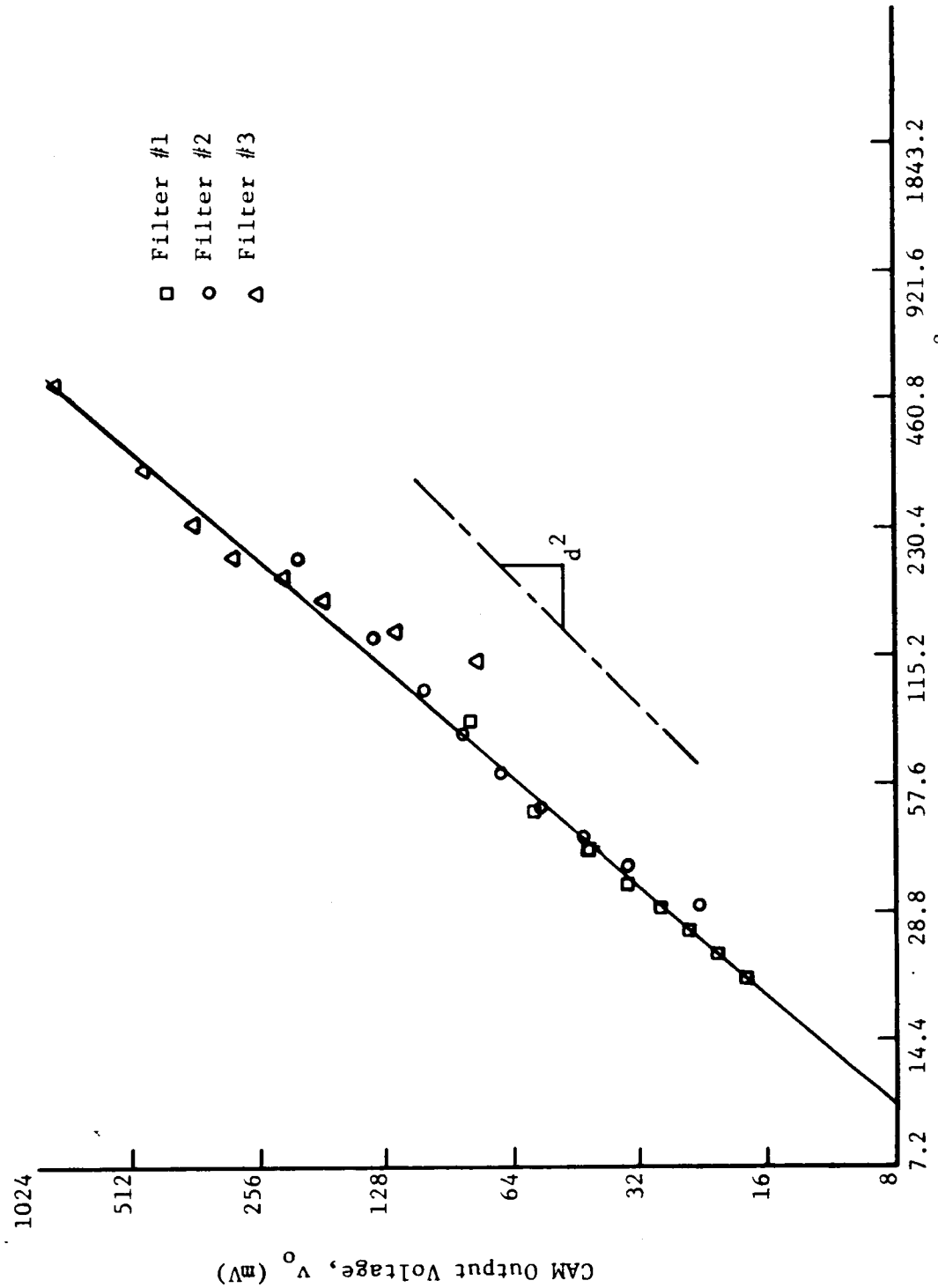


Figure 4-4. System calibration by penetration efficiency method.

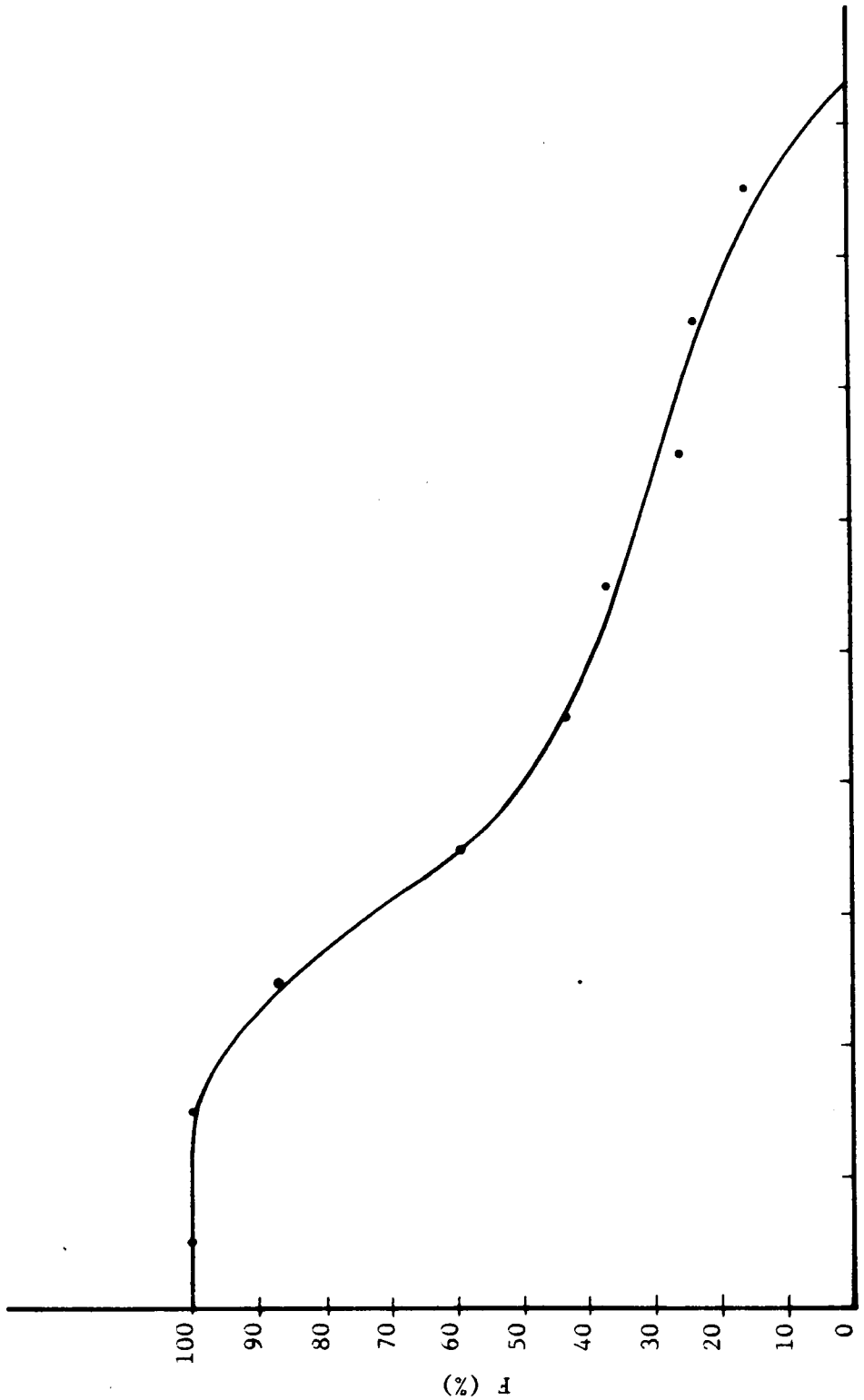


Figure 4-5. Vertical elutriator penetration efficiency function by CAM output data.

which is significantly lower than the theoretical value of 15 μm. Bethea and Morey reported a Stokes settling diameter of 12 μm for the full size vertical elutriator operated at a flow rate of 7.4 ℓ/min. It is important to note that the CAM calibration is based on an equivalent projected diameter and not the true Stokes diameter. Since, in general, the Stokes diameter is greater than or equal to the equivalent mean projected diameter, it is expected that the predicted elutriator cutoff will read low.

The results of microscopy are shown in Figure 4-6. It is seen that the VE cutoff occurs at a projected diameter of 10.8 μm. This value is in good agreement with the CAM predicted value of 11.8 μm. The extended tail of the VE penetration efficiency curve indicates that it is not a simple function of the equivalent projected diameter alone. Apparently, the particle shape as well as the size determines the VE response.

The raw data used to compute the VE penetration efficiency curve of Figure 4-6 may be reorganized to determine the VE response to maximum and minimum particle dimensions. The number distributions $p(d_M)$ and $p(d_m)$ are determined for both CAM runs and the resulting penetration efficiencies are then computed. The results are shown in Figure 4-7. It is immediately evident that the vertical elutriator responds more to the particle minor dimension than the major dimension. The minor dimension penetration efficiency function is seen to exhibit typical characteristics, with a 50% cutoff diameter of about 9 μm.

The major dimension penetration efficiency curve is quite different in that the function does not decrease montonically. It was

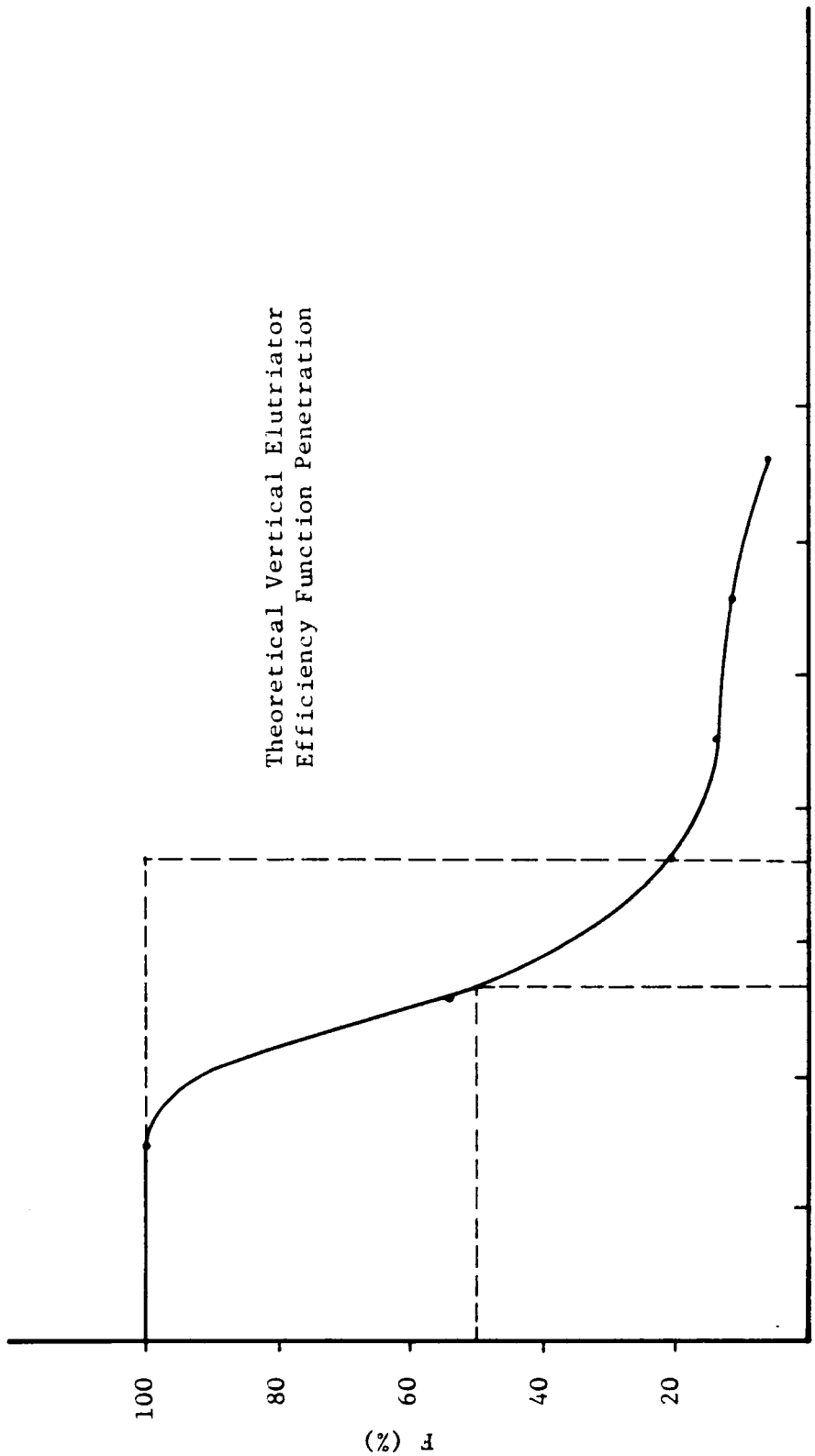


Figure 4-6. Vertical elutriator penetration efficiency function by optical microscopy.

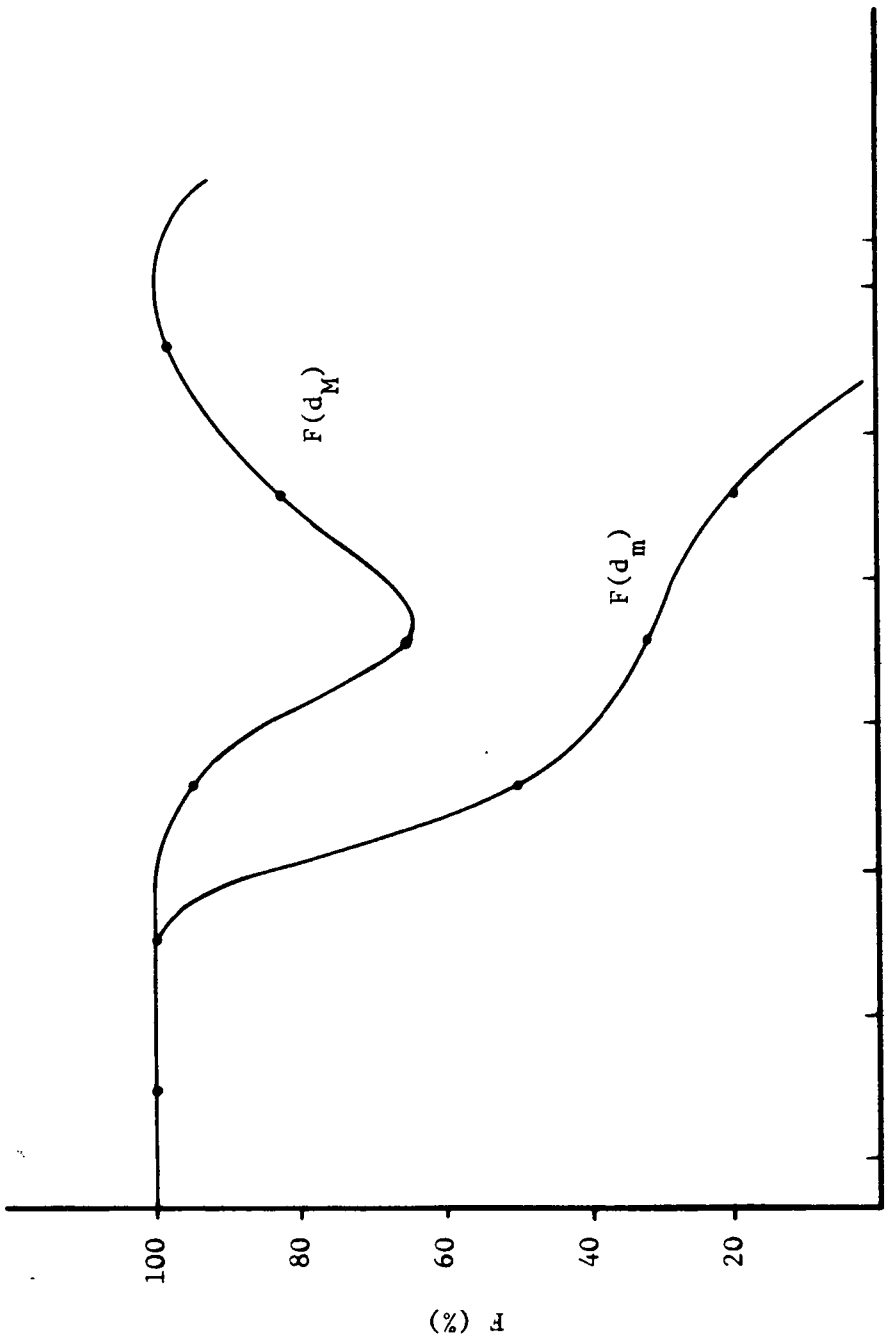


Figure 4-7. Vertical elutriator penetration efficiency for maximum and minimum particle dimensions.

observed that the vast majority of particles with dimensions greater than 20 μm are cylindrical rods with aspect ratios greater than about 5. Therefore, it may be hypothesized that the major dimension penetration efficiency curve is actually a combination of two separate phenomena. For dimensions less than about 10 μm, the particle distributions are predominantly composed of roughly spherical or compact particles, and the typical penetration efficiency function behavior is observed. However, at larger dimensions, the number of fibers is much greater than the steadily decreasing number of compact particles and so dominate the penetration efficiency function. Although the true equivalent Stokes diameter is dependent upon both dimensions, it appears that the minor dimension dominates the vertical elutrator response.

CAM Mass Calibration

The system calibration shown in Figure 4-4, page 41, may be interpreted as the average CAM response to a given size particle. If the particles were all spherical and of known composition and if the CAM counting efficiency as well as the calibration curve were very accurately known, then the mass distribution could be easily computed from the predicted number distribution. Unfortunately, this procedure usually works very poorly for all optical counters, even for well-characterized particles, and it is highly dubious for irregular, large particles of cotton dust, whose composition is variable. The mass distribution which is of prime importance to the industrial hygienist may be determined through an alternate technique, in the unique case of the CAM sensor.

Recall that the CAM is implicitly calibrated such that with large particle compensation its readings are made to agree well with the VE. This is the primary objective for the CAM, and whether this implicitly determined calibration agrees with an explicitly determined result is somewhat secondary. Indeed, the results will generally be different to compensate for subtleties in the equipment and to accommodate the variations of particle characteristics encountered in practice.

The approach in this second method was to assume the implicit CAM calibration to be perfect and then to compute the differential mass directly from the pulse height distribution, thus leading to differential mass for each CAM channel. These data were then compared with microscopy data for which differential masses versus average projected area were computed as described in the previous chapter.

It is evident that the approach to system calibration based on mass response is inherently different than the previously determined size calibration from penetration efficiency experiments. It is noted that this calibration is sensitively dependent on the details of the implicit algorithm, which are proprietory. However, the concept of compensation has been described in Chapter II, and a general explanation may be given to facilitate understanding the results.

It was found through numerous system calibration tests that a linear large particle compensation algorithm was optimum in predicting total mass of cotton dust. This rather profound finding implies a simple relationship between large particle volume and projected area.

For the theoretical case of a distribution of spherical particles, it has been shown that the voltage response to very large particles is

proportional to the projected area. It is deduced that the large particle volume (or mass) would be proportional to the output voltage raised to the 3/2 power. A compensation algorithm utilizing a function of the form

$$V = \kappa \Delta v^{3/2} \tag{4-1}$$

could be implemented in the CAM microprocessor in order to correct for the inherent underweighing of large particles. For cotton dust, it was determined that this form of large particle compensation consistently overweighed the actual mass, and accordingly, a smaller exponent was required. Apparently for large cotton dust particles, which are predominantly fibrous, a linear function gives a surprisingly close approximation to the actual particle mass. This result implies that, on the average, the fiber volume is directly proportional to the projected area. One conclusion is that the fiber diameter remains relatively constant, while the length may vary considerably. Fiber tenacity studies give geometrical parameters that support this theory (21).

It is theorized that for large cotton dust particles, the mass is proportional to the projected area which, in turn, is proportional to the output voltage produced. Thus, by adjusting the system gain, the height of a particular voltage pulse may well be interpreted as the mass of the particle that caused that response. The mass associated with the particles registered in any PHA channel is therefore found by summing the individual pulse magnitudes and multiplying the total by some system gain factor. In the CAM System, the pulse height analyzer only stores

numbers of counts and not individual pulse amplitudes, an average pulse height is determined for each channel. Thus, the CAM mass distribution may be envisioned as a series of monodisperse distributions which contain the large particle mass fractions. The resulting PHA histogram predicted by the CAM System was then correlated to the true mass distribution derived from microscopy.

It was also found in the initial equivalency tests that the size distributions vary considerably between different cotton manufacturing processes. Representative CAM PHA histograms are shown in Figure 4-8 for each of three processes. The percentage of mass associated with large particle data is found by integrating or summing the nine histogram cells. Note that while the winding and opening histograms contain approximately the same fraction of total mass, the histogram shapes are quite different. The carding histogram is similar to the winding histogram except that the values are smaller.

The three corresponding mass histograms determined through microscopy are shown in Figure 4-9. It is immediately evident that the tails of the distributions are similar to the corresponding CAM histograms of Figure 4-8. Instead of trying to correlate the two distributions directly, it is somewhat more exact to compare the corresponding cumulative mass distributions. The mass histograms of Figure 4-9 are summed from the "top down," and the cumulative distributions are shown in Figure 4-10. The ordinate represents the equivalent projected diameter, and the abscissa is interpreted as the percentage of mass above the corresponding particle size. The mass mean diameter is read directly by locating the 50% point. The mass mean diameters all fall



Figure 4-8. Mass histograms from CAM PHA data.

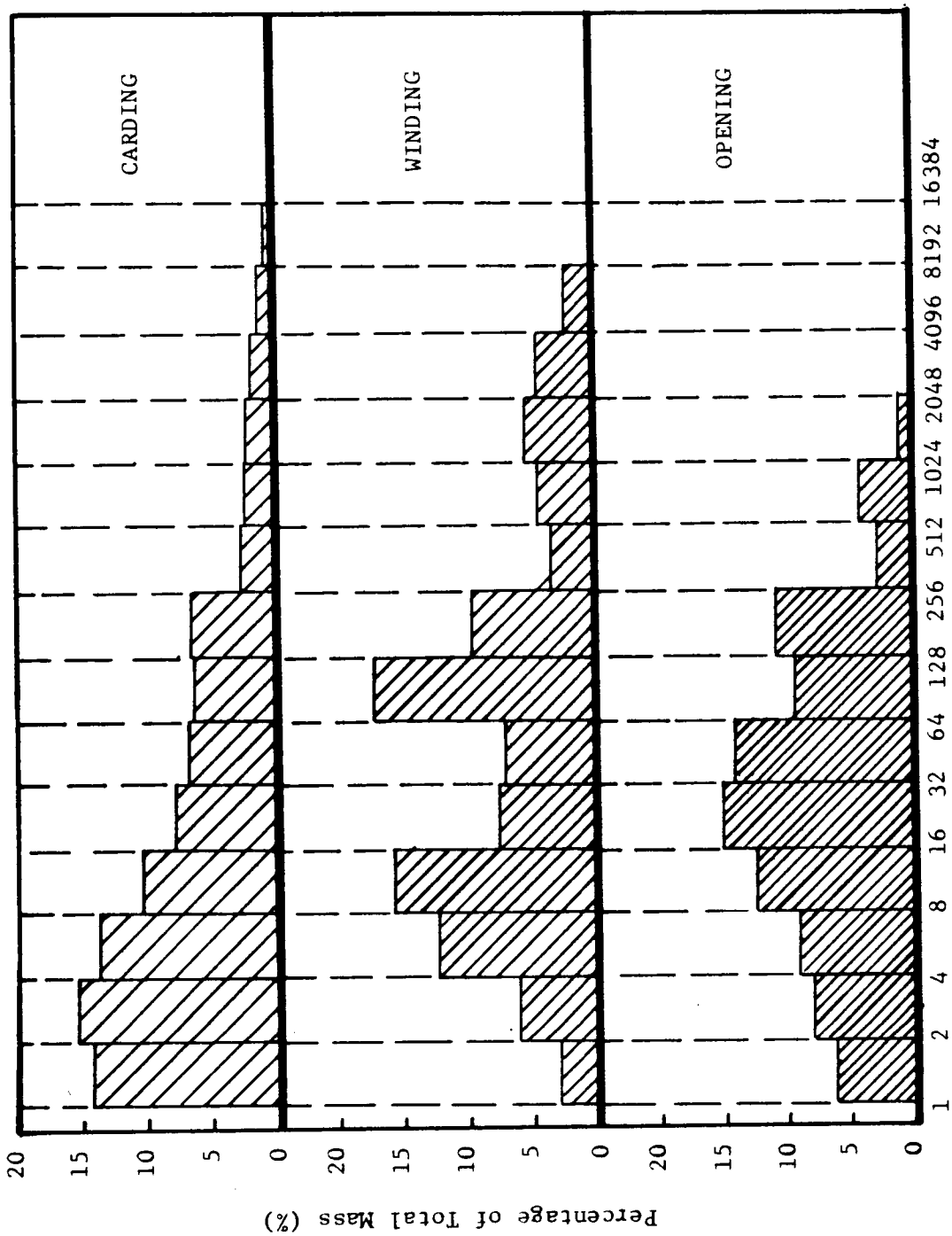


Figure 4-9. Mass histograms from optical microscopy.

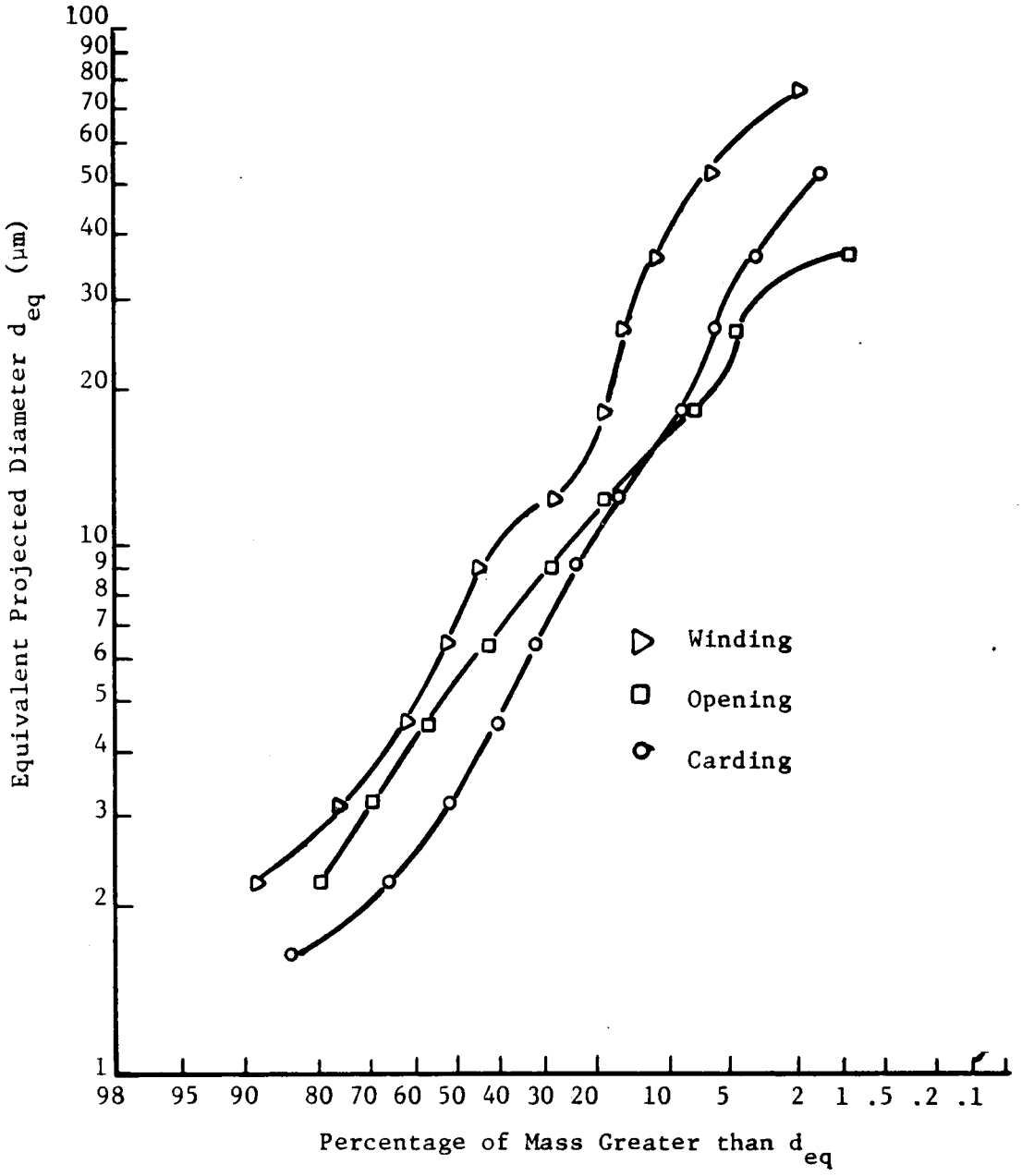


Figure 4-10. Comulative mass distributions by optical microscopy.

within the range 3-7 μm which agrees reasonably well with previously published data (11).

The CAM PHA distribution is treated in the same manner, and the results are given in Figure 4-11. The values indicated by Figure 4-11 are treated as the independent variable, and the corresponding particle diameter is treated as the dependent variable. For example, from Figure 4-11 it is seen that for the winding process, 7% of the total mass is expected to occur in and above channel seven. The corresponding cumulative mass distribution in Figure 4-10 indicates that 7% of the total mass is found in particles with equivalent projected diameters greater than about 48 μm. Thus, it may be said that on a mass basis the lower boundary of channel seven corresponds to a particle projected diameter of 48 μm. The same procedure is applied for each PHA channel, and the results are tabulated in Table 4-1.

The average channel boundaries are computed, and the data are plotted in Figure 4-12, which represents the system calibration on a mass basis. A linear curve fit gives a channel calibration with an accuracy of better than ±20% of the actual experimental function. This linear approximation to the system calibration gives a slope that is within 1% of the theoretical case based on a d^2 relationship.

Nonrespirable dust or the large particle fraction (LPF), which should be excluded in cotton dust measurements, is associated with particles with aerodynamic diameters greater than 15 μm. From the system calibration on a mass basis, it is seen that according to the definition of "respirable" dust all PHA counts occurring above channel two contribute to the LPF. For the three processes under examination,

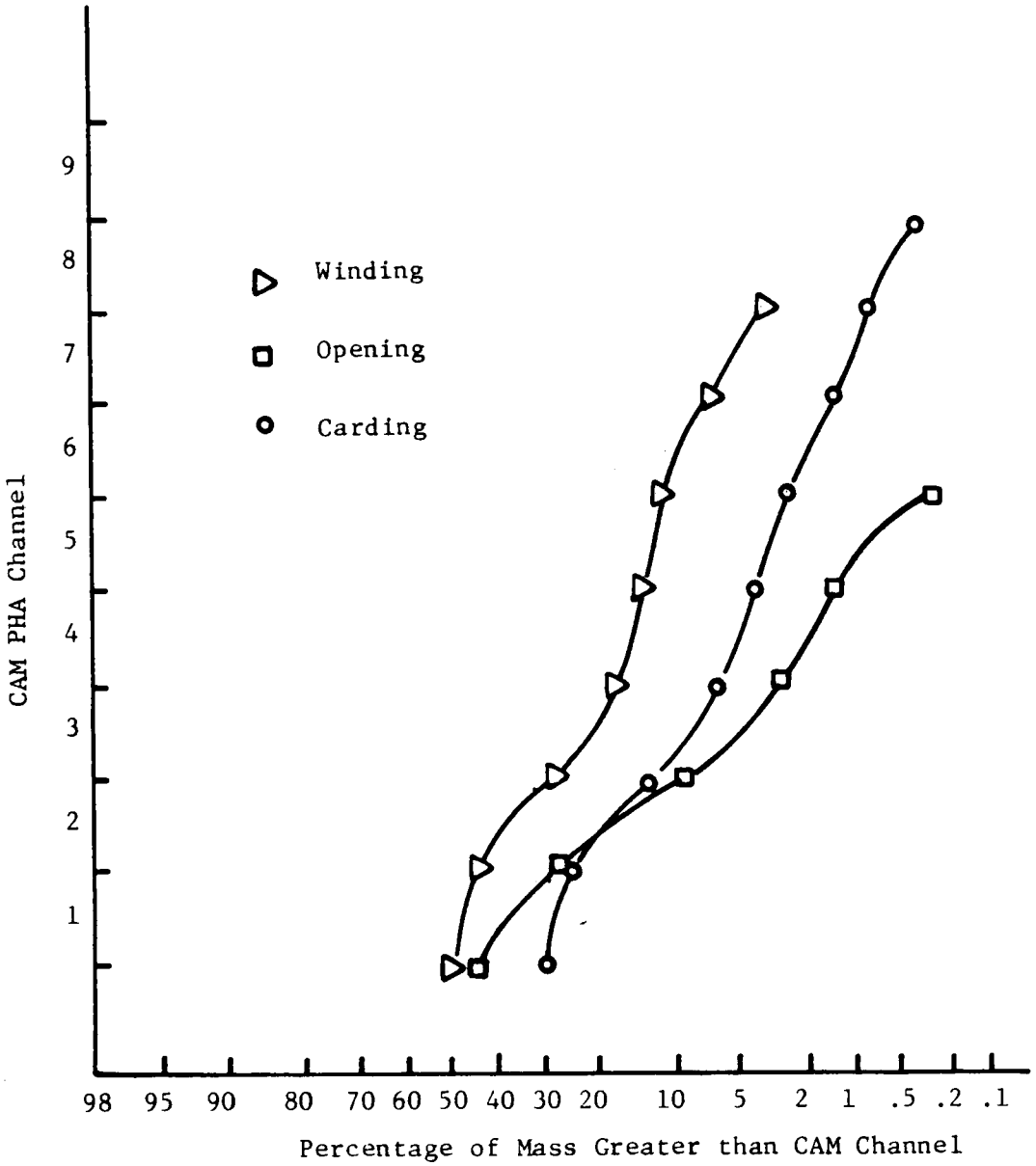


Figure 4-11. Cumulative CAM PHA distribution.

Table 4-1. Channel boundaries determined on a cumulative mass basis.

PHA Channel Number	Equivalent Projected Diameter of Lower Channel Boundard (μm)			
	Carding	Winding	Opening	Average
1	7.2	7.0	5.8	6.7
2	9.0	9.6	9.9	9.5
3	14.5	12.5	17.1	14.7
4	24.5	20.0	28.0	24.2
5	32.0	30.0	35.0	32.3
6	40.0	37.0	--	38.5
7	52.0	48.0	--	50.0
8	61.0	63.0	--	62.0
9	80.0	--	--	80.0

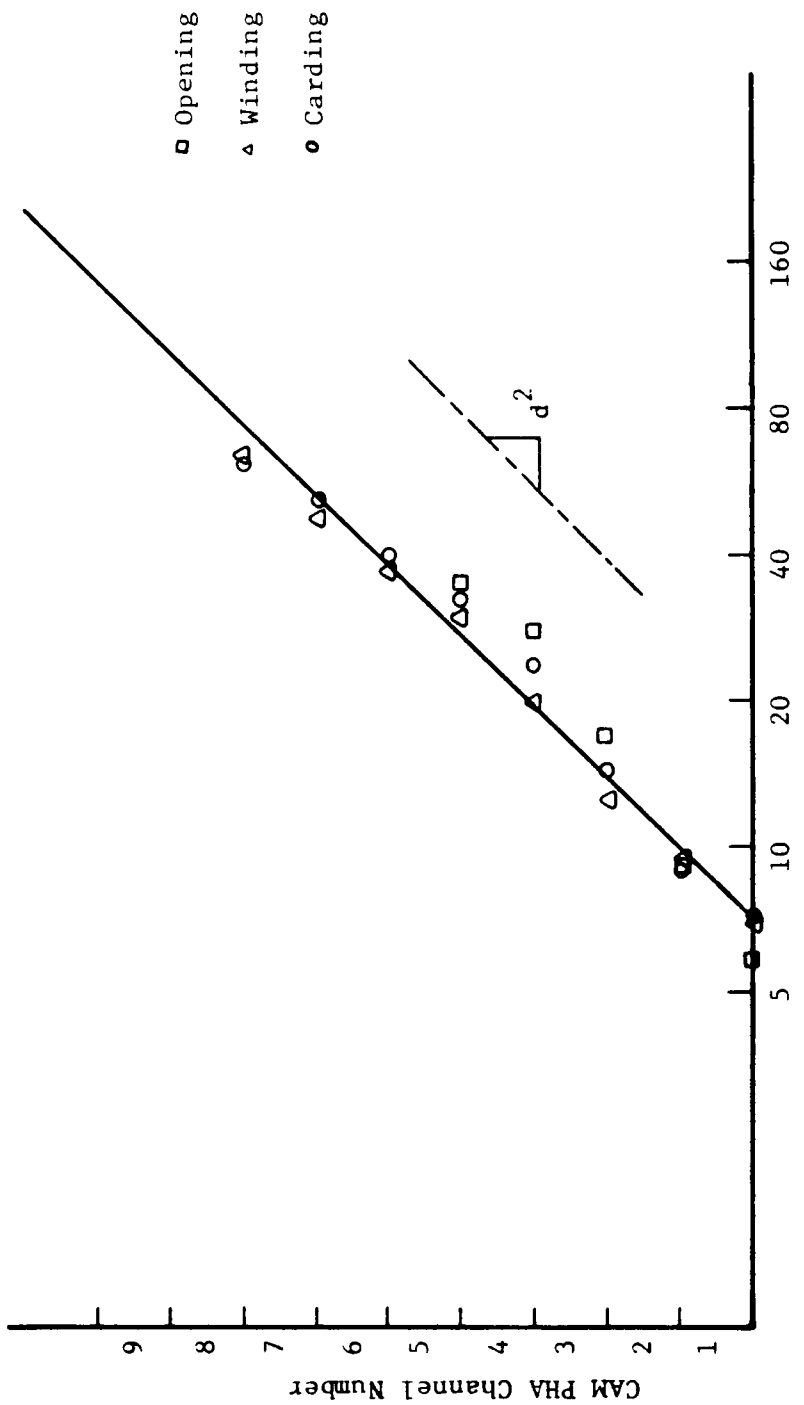


Figure 4-12. CAM PHA channel calibration on a mass basis.

the large particle fraction ranges from about 9% (opening) to over 28% (winding).

The mass calibration result is used in practice because it directly addresses the explicit determination of large particle mass fractions, based on the standard algorithm. Also, this calibration gives a CAM counting efficiency which is in good agreement with expectations, as described next.

CAM Counting Efficiency

The CAM counting efficiency is defined as the ratio of particles counted by the CAM sensor to those counted on the filter microscopically. This is done on a particle class basis. The average collection efficiency histogram shown in Figure 4-13 uses the mass basis system calibration in defining histogram class boundaries. For the middle-to-upper range channels, the value of collection efficiency remains at a fairly constant fraction of about 65%. Again, the reduced efficiency in the lower channels is attributable to coincidence counts due to increased count rates.

Instead of relating the CAM counting efficiency to the PHA channels for typical processes, it is perhaps more revealing to examine the count rate dependence. The PHA channel counts data may be time normalized so that variations in mass concentrations between processes is eliminated. Thus, in Figure 4-14, the CAM collection efficiency η is plotted against the count rate in particles per minute. It is seen that for count rates less than about 100/min the sampling efficiency is relatively constant at about 70%. For rates greater than 100/min, the

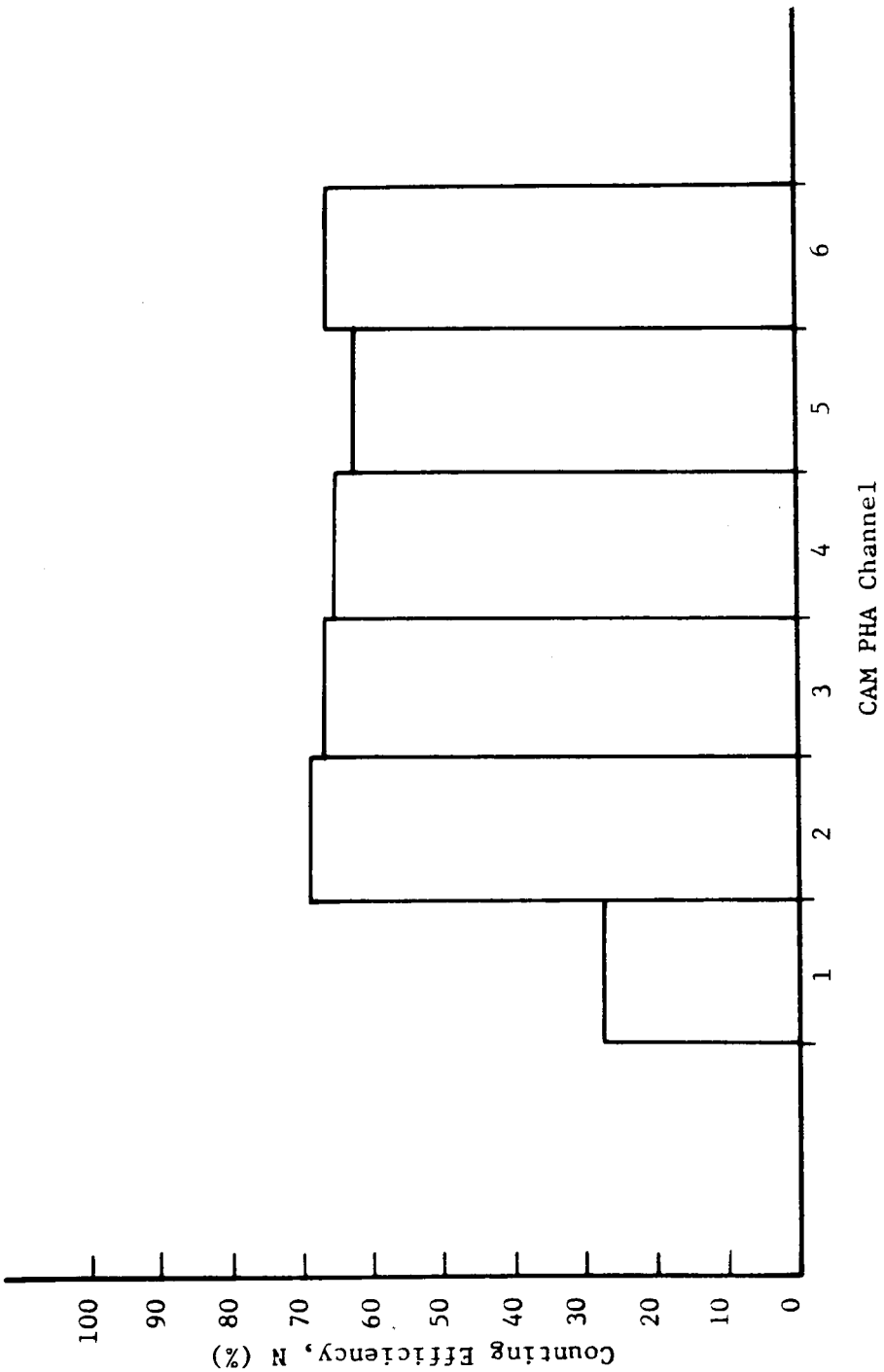


Figure 4-13. CAM counting efficiency vs. PHA channel.

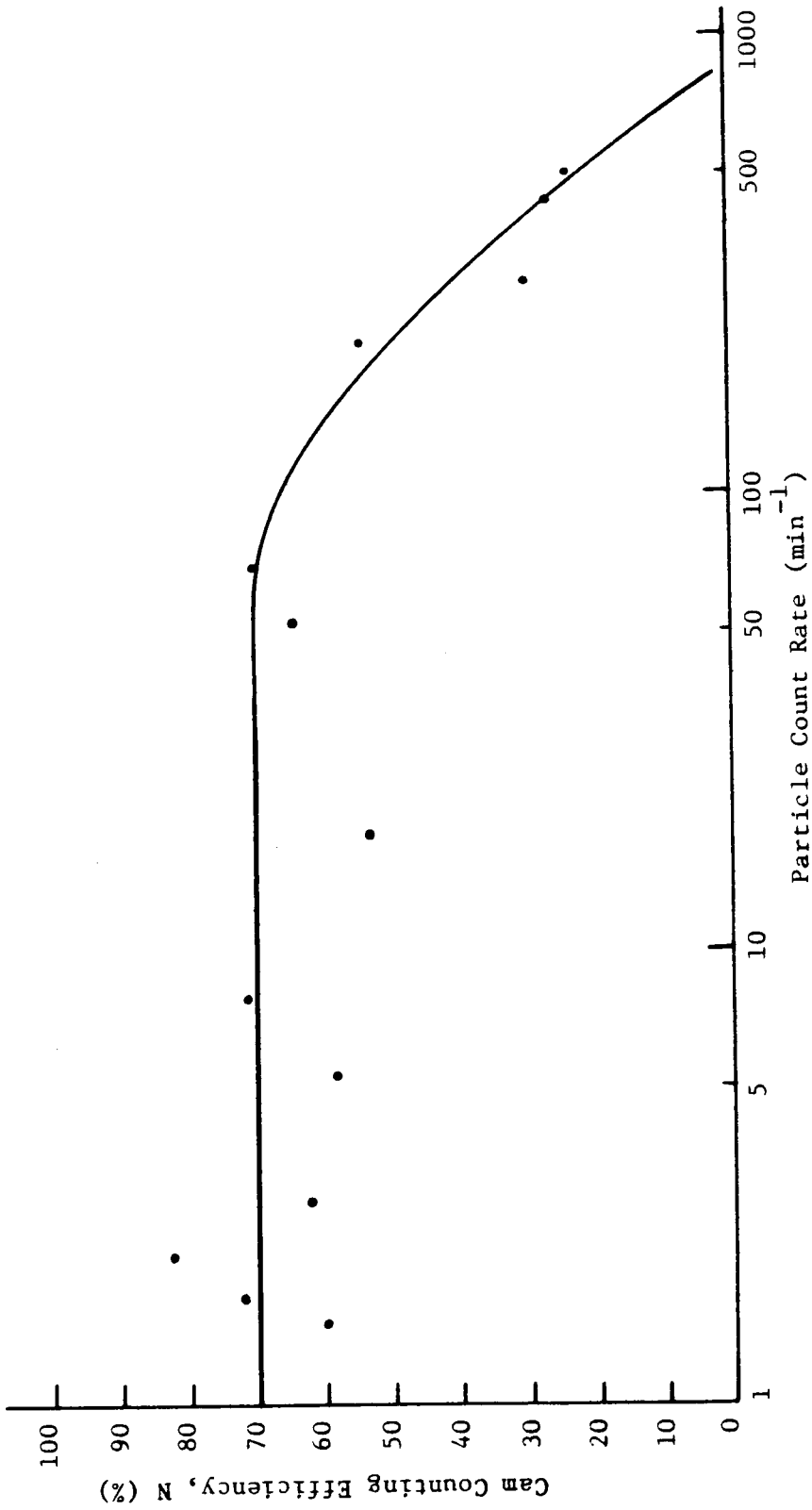


Figure 4-14. CAM counting efficiency vs. particle count rate.

function rolls off monotonically as would be expected. It should be noted that this function does not include the size dependent variable as a parameter. In other words, this determination does not deal with variations in coincidence counts due to particle size alone. Intuitively, for equal count rates, two 10 μm particles have a greater probability of coincidence than two 1 μm particles. However, for the processes under study, it is seen that, on the average, sampling efficiency is independent of count rate for rates less than about 100/min.

Volume to Area Ratio

It was determined experimentally that for large cotton dust particles a linear relationship between particle volume and projected area exists. The consistency of calibration results indicate that indeed, on the average, the particle volume to area ratio approaches a constant value. The results of microscopy can be manipulated to test this hypothesis. Using the raw dimensional data, the approximate volume to area ratio is computed for each sampled particle. Grouping by projected area, the V/A histogram is formed by computing the mean V/A ratio for each interval. The results are given in Figure 4-15, showing the size dependence of the V/A ratio. For the theoretical case of solid spherical particles, the volume to area ratio increases as the diameter as indicated by the superimposed curve. This function represents the extreme case as the sphere is the most compact of all geometrical shapes. Accordingly, all other shapes possess smaller V/A ratios as is seen in the experimental data. Note that for small cotton dust particles the V/A relationship approaches the spherical case. As the projected

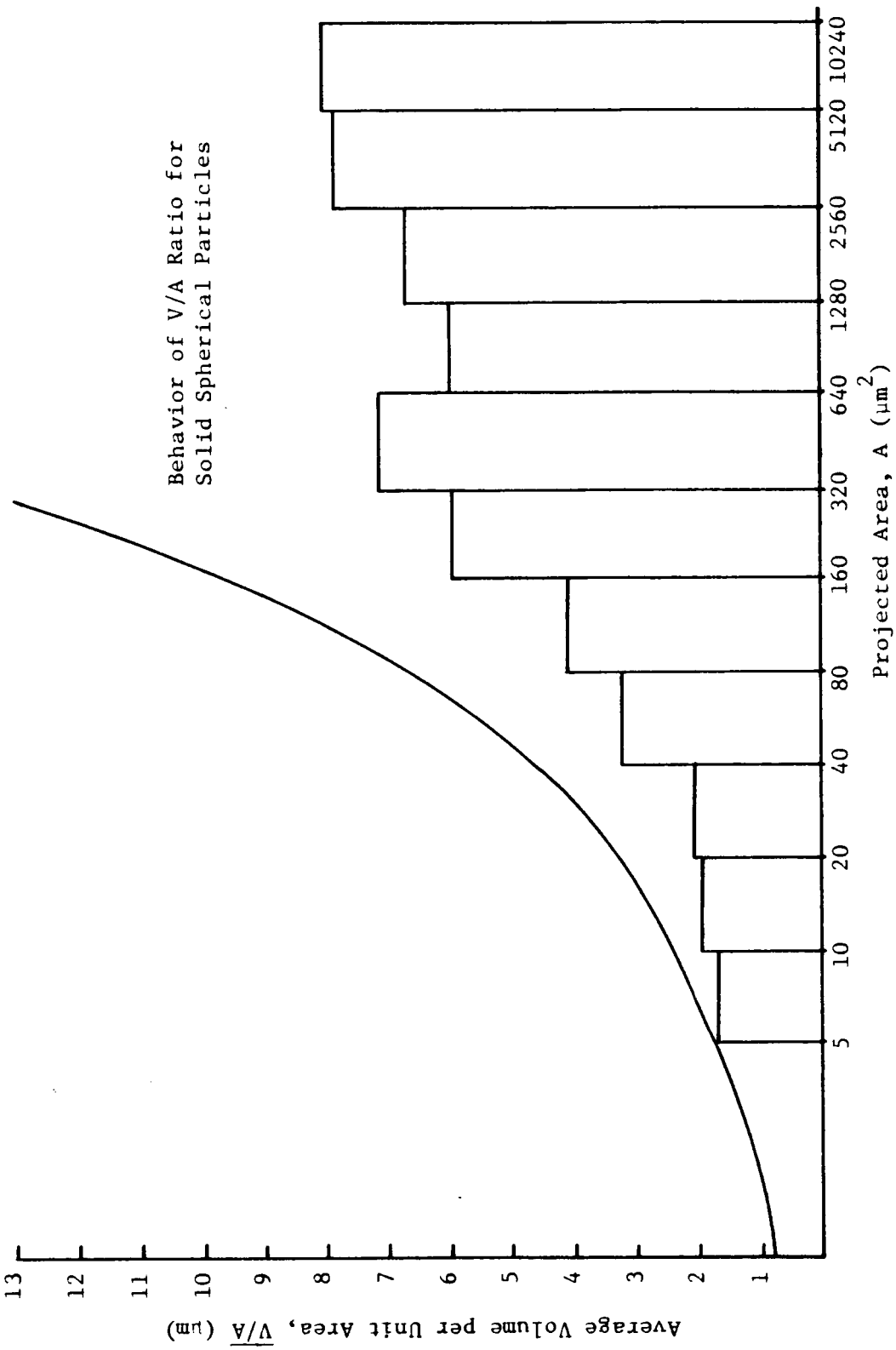


Figure 4-15. Average volume to area ratio for cotton dust.

area increases, the V/A ratio increases to a maximum value that remains relatively constant. In general, the increasing particle elongation accounts for the increasing deviation from the spherical case. For very large particles, above 300 μm^2 in projected area, the geometry is predominantly cylindrical, and the V/A ratio is proportional to the fiber diameter. Therefore, from Figure 4-15, it is evident that the fiber diameter reaches a maximum dimension that is independent of fiber length. Apparently, this unique feature of cotton dust allows a linear approximation in relating large particle mass to optical scattering yield.

CHAPTER V

SUMMARY AND CONCLUSIONS

The main thrust of this research has been to explicitly calibrate the CAM instrument. The experimental procedure was based on comparison of simultaneous CAM PHA output data and microscopically determined particle size data. Average values of input and output data were determined and results were correlated.

The calibration data were obtained by running CAM tests in the mill environment. CAM output data were recorded and corresponding particle size information was determined through microscopic analysis.

A technique of equal area sampling was utilized in determining particle size distributions from optical microscopy. By choosing the sample points in such a manner, the data could be used to form a size distribution directly without requiring weighting factors. The resulting projected area distributions were used in determining the system calibration on a number basis.

The calibration based on particle numbers utilized a differential technique in relating input-output data. Factors such as variable fiber orientation and unknown system collection efficiency precluded an absolute calibration. By working with differential changes, these variables were hopefully cancelled or neutralized. The term "average" must be emphasized as being imperative in interpreting the calibration results. Specifically, the projected area of a typical long fiber can vary over more than two orders of magnitude due to orientation alone, causing vast differences in optical scattering response. Thus, mean

values must be utilized since individual responses cannot be reasonably determined.

The differential technique of number calibration was implemented by perturbing a known size distribution with a filtering device and interpreting the change in input and output data. The penetration efficiency of the filter was determined by both CAM output data and optical microscopy, and the two resulting functions were compared to give transfer characteristics of the CAM sensor. By choosing materials with varying penetration efficiency functions, a wide range of input-output data was obtained, and the CAM System calibration on a number basis was determined.

The vertical elutriator penetration efficiency function was also used as a test of the calibration results. The results were in good agreement with the previously determined calibration results. The VE microscopy data were also used to characterize the particle shape response of the vertical elutriator. It was found that the particle smallest dimension dominated the VE penetration efficiency function. This finding verifies the assumption that the VE does not completely reject non-respirable particles.

The empirical CAM mass concentration algorithm was used to compute an estimate of the mass distribution of large cotton dust particles. Microscopic measurements were used to calculate a corresponding mass distribution which was assumed to be reasonably accurate. The cumulative mass distribution was then normalized and compared to the CAM PHA distribution giving a system calibration on a mass basis.

Both of the system calibrations gave linear slopes in agreement with theoretical considerations. The calibration based on penetration

efficiency is interpreted as the average CAM voltage response to an arbitrary size particle regardless of source. The mass calibration is based on the CAM large particle compensation algorithm for cotton dust particles and must be interpreted as such.

Several assumptions were utilized in the determination of the CAM system calibration on a mass basis. First, the mass distributions derived from optical microscopy were based on approximate particle geometrical properties. The assumption of a constant V/A ratio was shown to be accurate for very large particles (fibers), but considerable errors could result in the lower channels due to this approximation. In addition, the CAM counting efficiency has an effect on the predicted mass distribution and could be responsible for nonlinearities in the mass calibration curve. Considering the large number of variables, the results are regarded as good.

In summary, two fundamentally different calibration results were obtained. The number calibration by the penetration efficiency method verified the theoretical relationship between average, large particle size and CAM voltage response.

Using the result that CAM response is proportional to d^2 plus the assumption of a simple relationship between large particle volume and average projected area, the concept of large particle mass compensation, which was previously implemented through an empirical algorithm, was evaluated.

In the CAM mass calibration, this algorithm was assumed to be correct, and the results were compared to the microscopically determined particle mass distributions. The practical application of this

calibration is in the determination of differential mass fractions. This is the most important result of the research as the CAM system is intended to give only two major pieces of data: the total mass concentration of particles and the portion of this mass that is associated with particles larger than a specified size.

LIST OF REFERENCES

LIST OF REFERENCES

1. Merchant, J. A.; Lumsden, J. C.; Kilburn, K. H.; O'Fallon, W. M.; Ujda, J. R.; Germino, V. H.; Hamilton, J. D. "Dose Response Studies in Cotton Textile Workers," Journal of Medicine, Volume 15, pp. 222-230; 1973.

2. "Occupational Exposure to Cotton Dust," Federal Register, Volume 43, No. 122, June 1978.

3. Neefus, J. D.; Lumsden, J. C.; Jones, M. T. "Cotton Dust Sampling, II--Vertical Elutriation," American Industrial Hygiene Journal, August 1977.

4. Lundgren, D. A.; Carter, L. D.; Daley, P. S. "Aerosol Mass Measurement Using Piezoelectric Crystal Sensors," Symposium on Fine Particles--Aerosol Generation, Measurement, Sampling, and Analysis. New York: Academic Press, Inc., 1976.

5. Macias, E. S., and Husar, R. B. "A Review of Atmospheric Particulate Mass Measurement via the Beta Attenuation Technique," Symposium on Fine Particles--Aerosol Generation, Measurement, Sampling, and Analysis. New York: Academic Press, Inc., 1976.

6. Shofner, F. M.; Miller, A. C.; Kreikebaum, G.; Kerlin, T. W.; Sasser, P. E. "Electro-Optical Measurement of Cotton Dust: An Equivalent Alternative to the Vertical Elutriator," Proceedings of Third Special Session on Cotton Dust, Beltwide Cotton Conference, Phoenix, Arizona, January 9-10, 1979.

7. Miller, A. C. Theoretical Modeling and Calibration for a Particulate Mass Concentration Monitor. M.S. Thesis, The University of Tennessee, Knoxville (1977).

8. Carlson, T. B. Design Considerations for Particulate Instrumentation Employing Laser Light Scattering. Ph.D. Dissertation, The University of Tennessee, Knoxville (1974).

9. Kerker, M. The Scattering of Light and Other Electromagnetic Radiation. New York: Academic Press, 1969.

10. Van de Hulst, H. C. Light Scattering by Small Particles. New York: John Wiley, 1957.

11. Shofner, F. M.; Kreikebaum, G.; Miller, A. C.; Kerlin, T. W. "Real Time, In Situ Electro-Optical Measurement of Dust Parameters," presented at the International Symposium on Grain Dust, October 2-4, 1969, Manhattan, Kansas.

12. Fornes, R. E.; Kleinfelter, M. M.; Hersh, S. P. "Particle Size Analysis of Cotton Dust Using Scanning Electron Microscopy," Proceedings of the Textile Engineering Conference, The American Society of Mechanical Engineers, September 1976.

13. Irani, R. R.; Callis, C. F. Particle Size: Measurement, Interpretation, and Application. New York: John Wiley, 1963.

14. Stockham, J. D., and Fochtman, E. G. Particle Size Analysis. Ann Arbor, Michigan: Ann Arbor Science Publishers, Inc., 1977.

15. Hatcher, J. D. "Physical Characteristics of Cotton Dust Generated in Different Processing Areas of a Cotton Mill," Proceedings of a Topical Symposium on Cotton Dust, American Conference of Governmental Industrial Hygienists, November 1974.

16. Bethea, R. M., and Morey, P. R. "Effect of Operational Parameters on Vertical Elutriator Performance for Cotton Dust Sampling," Proceedings of a Topical Symposium on Cotton Dust, American Conference of Governmental Industrial Hygienists, November 1974.

17. Herdan, G. Small Particle Statistics. London: Academic Press, Inc., 1960.

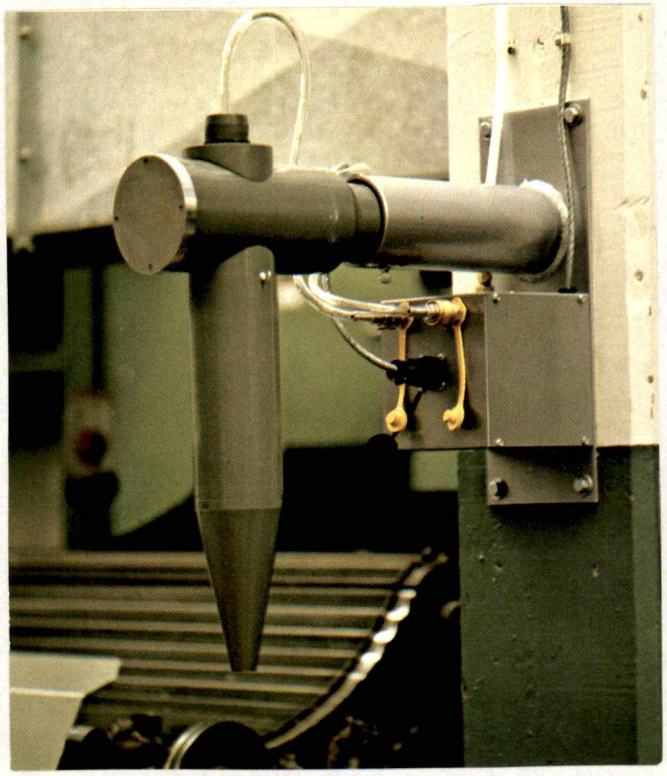
18. Johnson, L. J., and Leone, F. C. Statistics and Experimental Design. New York: John Wiley & Sons, 1977.

19. Heywood, H. "The Scope of Particle Size Analysis and Standardization," Symposium on Particle Size Analysis, Institution of Chemical Engineers, February 1947.

20. Harris, R. L., and Fraser, D. A. "A Model for Deposition of Fibers in the Human Respiratory System," American Industrial Hygiene Association Journal, February 1976.

21. Duckett, K. E. "Cotton Fiber Convolutions--Their Measurement and Relation to Fiber Tenacity," Tennessee Farm and Home Science, Agricultural Experiment Station of The University of Tennessee, Knoxville, Progress Report No. 102, 1977.

APPENDIX



A. CAM electro-optical sensor



B. Control/readout unit

Figure A-1. CAM sensor and control/readout unit.

VITA

Thomas Wesley Kerlin III was born in Columbia, South Carolina, August 15, 1955. He moved to Knoxville, Tennessee, at an early age where he attended Pleasant Ridge Elementary School and Farragut High School, graduating in May 1973. In September 1973, he enrolled at The University of Tennessee, Knoxville, in the School of Engineering. He participated in the Cooperative Engineering Program with the Union Carbide Corporation in Oak Ridge, Tennessee.

Upon graduation in June 1978 with a Bachelor of Science in Electrical Engineering, he began work on a Master's Degree with the research funded by PPM, Inc., of Knoxville, Tennessee. He accepted a teaching assistantship at The University of Tennessee, Knoxville, in September 1978 and completed his course work required for a Master of Science degree in Electrical Engineering in March 1980.

He is married to the former Candice Kay Eagle of Knoxville, Tennessee.